December 2017

Modifications to commercial printers to enable multi-material fabrication of 3D cellular scaffolds

Lucas D. Albrecht
Syracuse University

The scarcity of organs for patients that need transplants has led to exceedingly lengthy waits for organ transplants for sick patients. Fabrication of tissues and organ constructs *in-vitro* has potential to end the shortage, however many of the machines used to create these tissues and organs are expensive, not easy to use, and do not have any further practical applications. Bioprinting technology has the potential to revolutionize the fabrication of biological constructs that can be used as in vitro model tissues and vivo substitutes. Bioprinting is the process of using conventional 3D printing methods and computer-aided-design (CAD) to create patient and user specific constructs with biological material. 3D printers are ideal for low volume customizable parts, and when these parts can be made of living cells and biomaterials these machines become ideal for cell based research. Converting commercially available 3D printers into biomanufacturing units answers several problems that are faced by researchers, namely: the ability to create 3D multicomponent system creating multicellular interfaces in cell culture, and the ability to study cells in a true 3D environment. Although biological tissues have a range of cell types and material properties, current bioprinting methods are limited in their ability to print multiple materials simultaneously, especially tissues with vastly different material properties. For instance, printing of soft gels alongside a hard-structural material remains a challenge, as the thermal, mechanical, and biochemical parameters during the printing process must be maintained in an appropriate range to ensure high viability of living cells. Therefore, to truly realize the potential of bioprinting within the biomedical community, new capabilities that allow multi-material bioprinting are needed. The goal of this work is to enable four capabilities using commercially available inexpensive 3D printers: (i) printing of new thermoplastics, (ii) printing of structural thermoplastic material alongside soft biomaterials (iii) printing two soft biomaterials and/or cell types using conventional extrusion printing, and (iv) printing soft biomaterials that do

not possess the necessary material properties for conventional extrusion printing. Results from this work will democratize bioprinting technology by driving down the cost of entry into the field, and will enable its use in solving important challenges in the field of tissue engineering.

Modifications to commercial printers to enable multi-material fabrication of 3D cellular scaffolds

By:

Lucas Albrecht

B.S, Syracuse University, 2014

Thesis

Submitted in partial fulfillment for the degree of Master of Science in Bioengineering

Syracuse University
December 2017

Acknowledgements:

This work would not have been possible without the support from Pranav Soman, the Syracuse Biomaterials Institute, Alex Filip, Stephen Sawyer, the Syracuse University Student Machine shop, Richard “Dick” Chave, William “Bill” Dossert, Tim Breen, Katie Pierie, and Moriah D. Fickle. These persons and organizations helped me greatly and this could not have been done without all of their support.

Table of Contents

Chapter 1: Introduction

As of 2012, there were approximately 117,000 patients awaiting an organ transplant, while the number of donors available was about 14,000, and trends show the disparity between these two numbers is growing every year (*Organ Procurement and Transplantation Network. 2013*). Figure 1 illustrates this growing disparity between these two groups.

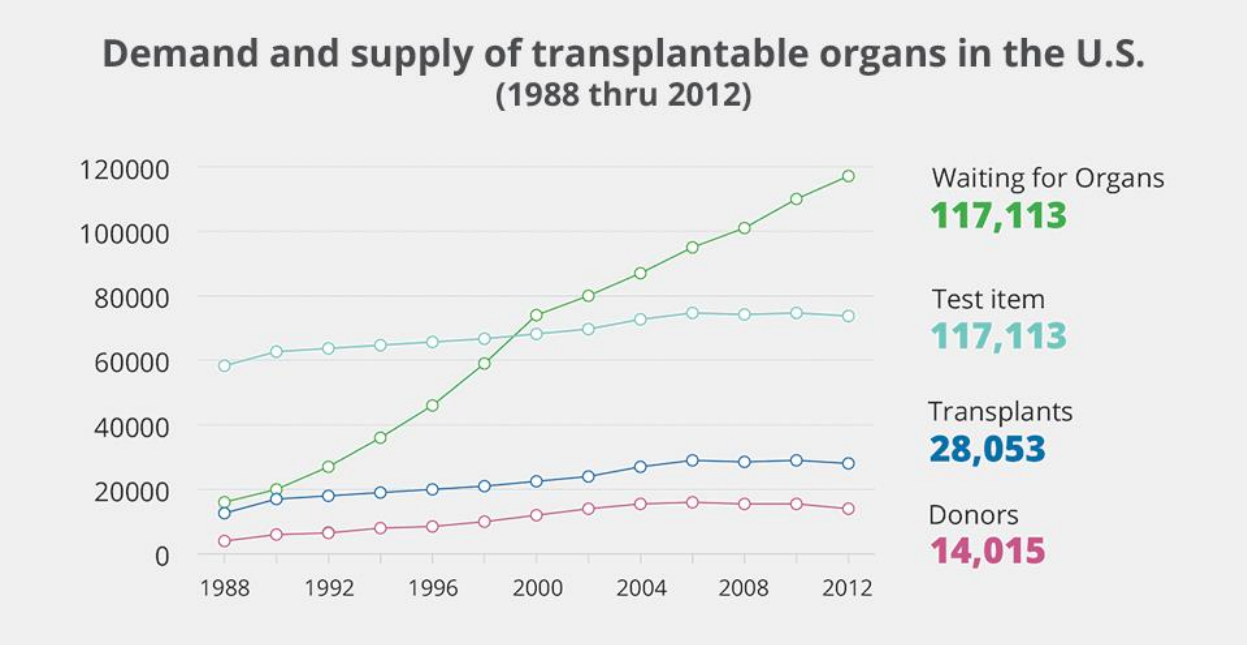

Figure 1: *Organ donors and recipients as of 2012 (Donors Matter).*

To mitigate this growing problem, an entire branch of engineering and science was created called tissue engineering. Tissue engineering is the use of cells, cell growth factors, and biocompatible materials to induce cell proliferation, tissue growth, and ultimately find a way to create functioning organs. An integral tool in assisting tissue engineering in recent years has been the use of 3D printers, as these machines are capable of creating user defined geometries with exact replication and limited human error. Though these machines have been used in the past, this paper will seek to find unique modalities to circumvent issues that previously presented problems in this field; for the purposes of making tissue engineering 3D printers much easier to

access, create, and use. In doing so we wish to lower the barrier of entry of using one of these printers and spur on this branch of research ultimately creating cellular constructs that are capable of supplementing many of the unmet needs of patients seeking a transplant.

1.1 3D Printing Technology

3D printing, also known as additive manufacturing (AM), is the process of creating parts/models by the addition of raw materials. 3D printing differs from typical manufacturing (machining) as these methods usually involve removing material to obtain a final product, instead of adding it. The benefits of AM being that these methods typically allow for greater user definition and rapid prototyping, while machining in particular has limitations in efficiency and is more costly. However, this tends to balance out when production shifts to mass scale, while the materials used in additive manufacturing have worse mechanical properties on average. AM can be applied in several ways: fused deposition modeling (**FDM**), stereolithography (**SLA**), **inkjet** printing, and fused laser sintering (**FLS**). Each of these methods makes use of a 3D CAD file and turns it into a solid object either by the addition of raw material, or accurate phase change in a user defined pattern. Each of these methods is a form of 3D printing and are similar with regards to what they accomplish, however, they all vary widely in the types of materials that they use, and the method by which they create finished products. Each printing method can be modified for bioprinting, with certain limiting factors for each method being what kinds of inks/materials are viable, and the ease of modification of each method when it is applied towards generating biomaterials.

In FDM printing a very precise nozzle is heated as a motor feeds in solid thermoplastic filament using the heat from the nozzle to melt the filament (**fig 2**).

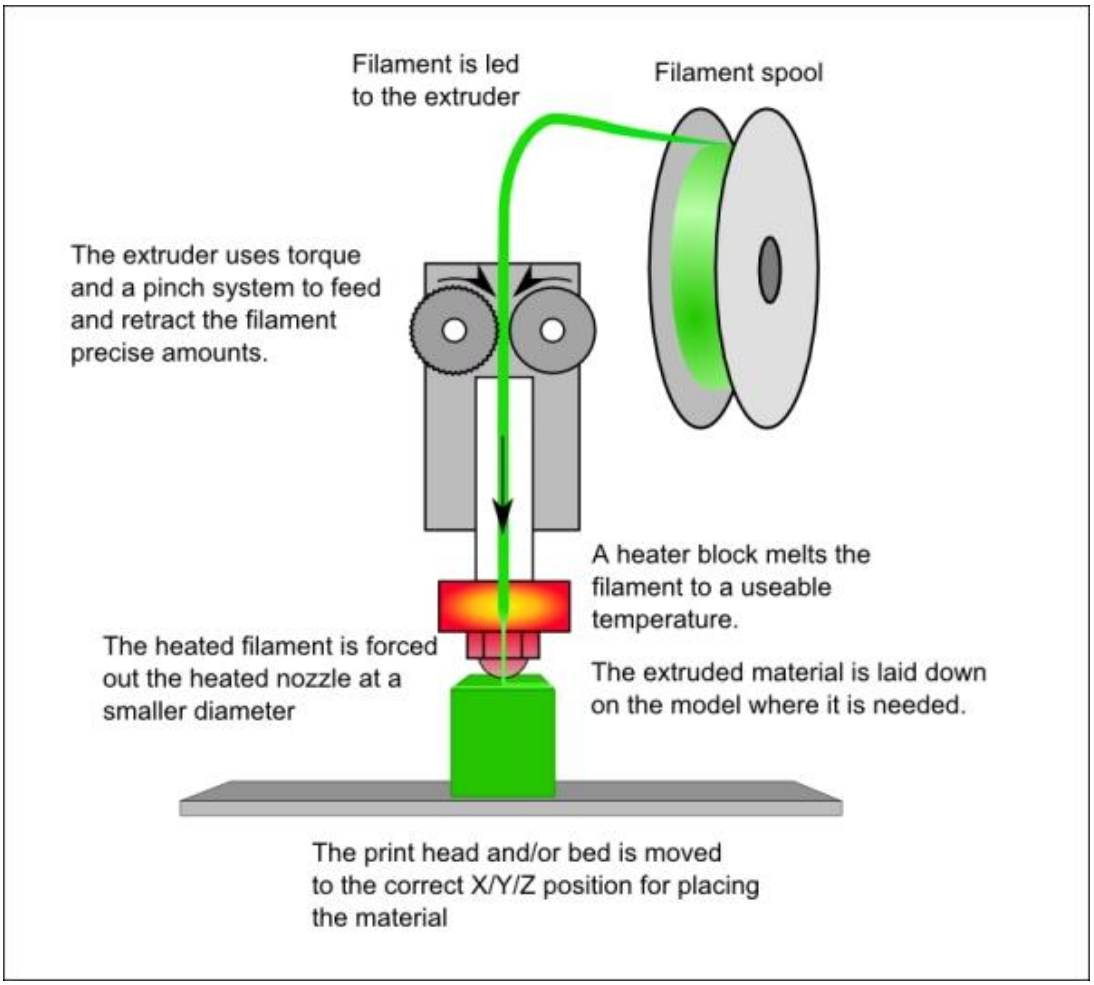

Figure 2: *Diagram of fused deposition model 3D printing, explaining the key mechanics of the process (Clone Inc.)*

The nozzle's inner diameter has such a close tolerance with the filament, that the solid filament creates a pressure extruding the melted material through the other end of the nozzle while the head and/or the build plate are moved in relation to one another, creating a solid object as the molten material cools and re-solidifies. The entire FDM process is driven by a single gear attached directly to a motor that feeds the solid material in during extrusion. FDM printing is governed by the principles of extrusion mechanics, therefore rheological effects of all extruded substances become paramount in resolution and cell viability during printing.

Stereolithography-based 3D printing uses a vertically moving platform, an ultraviolet light, a series of mirrors and lenses, and a bath of photo-reactive oxygen dependent polymer (**fig 3**).

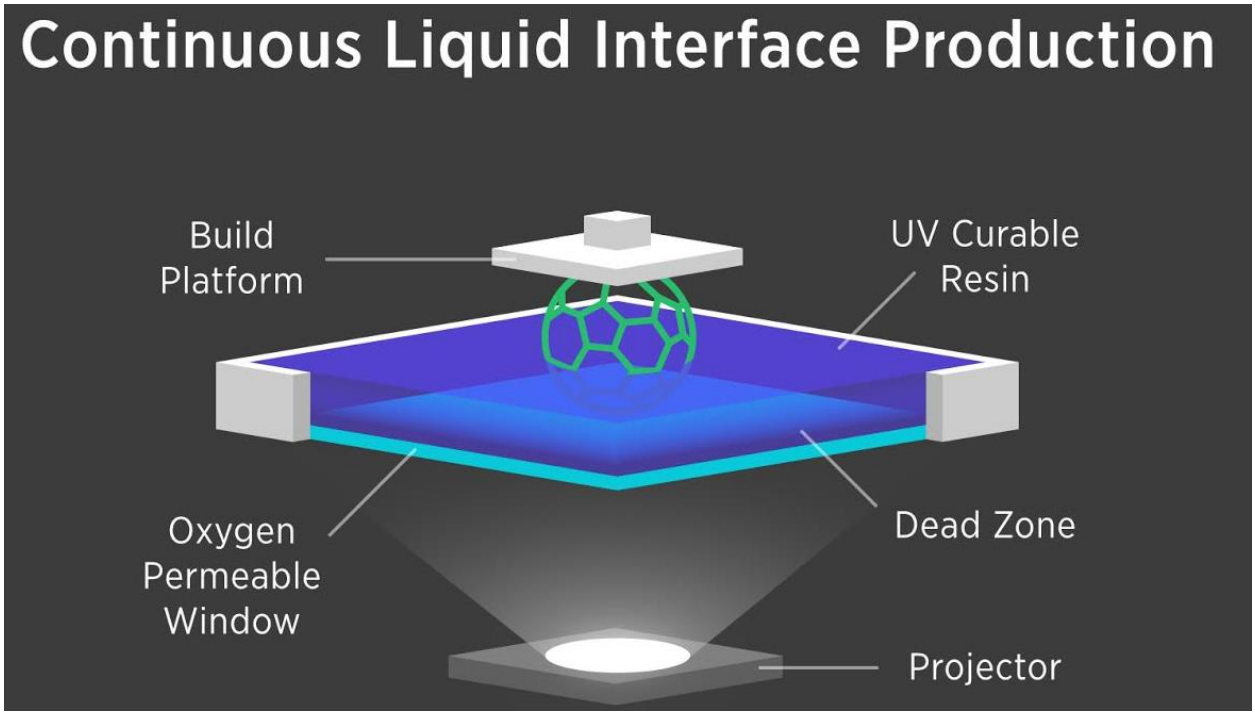

Figure 3: *Diagram of stereolithographic 3D printing (Makexyz).*

The polymer bath has a transparent window made that allows light to pass through. Light is projected from below the lense into the bath and onto the downward facing platform that is dipped into the bath. This method is different from other methods as the raw material is not being added, it's only changing phase. Since this method is dependent on light and there is no actual deposition of material SLA printing typically has very high resolution, and is very rapid. This method, however, has a lack in material choice, cell viability for bioprinting, and post processing. SLA prints need to be cleaned and post processed in alcohol (isopropyl), and then exposed to UV light for a longer amount of time to finish curing. As this applies to bioprinting, this presents a problem in that without finishing the curing process the material will not hold

form. Other labs have had difficulties using this method as large baths of photoreactive biomaterials cause cell death.

Inkjet bioprinting is the technique of using an inkjet printing head to expectorate nano-droplets of biomaterials and cells onto a two-dimensional surface and repeating this process to a given thickness (**Fig 4**).

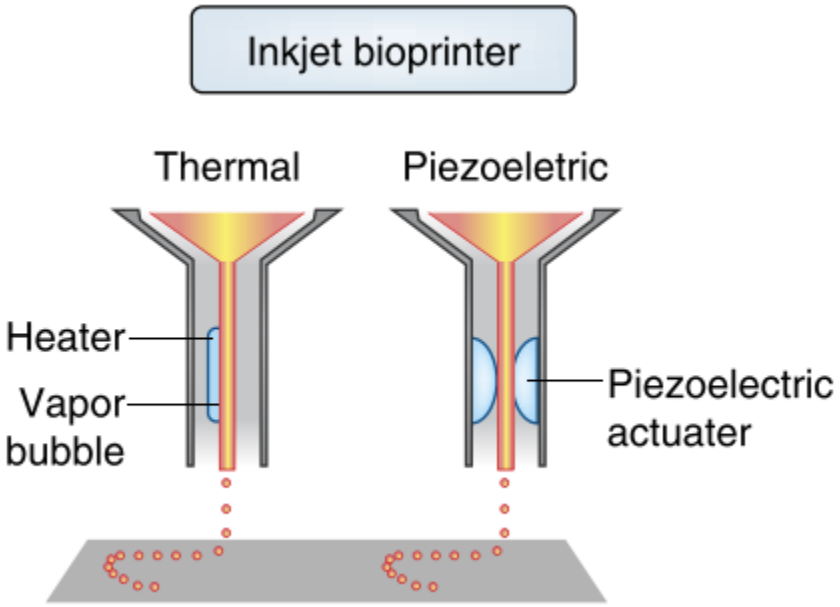

Figure 4: *A diagram of inkjet bioprinting using the thermal impulse and piezoelectric methods of actuation (labromancy.com)*

The inkjet head is composed of a reservoir, a nanoscale pore, and an element to apply impulse pressures. Impulse pressures can be applied via heating element, piezoelectric crystal, or an electromechanical valve. Heat based inkjet bioprinting uses a small element to induce a bubble to form and burst within the reservoir creating a pressure shockwave expectorating nano-spheres of biomaterial. This impulse heat can reach up to 300 degrees Celsius but lasts for approximately 2 nanoseconds leading to an overall maximum temperature change of 10 degrees and having minimal impact on cell viability (Mironov, V. "Organ Printing: Tissue Spheroids as Building Blocks." *National Center for Biotechnology Information*). This method allows for fast print speeds; however, it lacks directionality of droplet deposition, consistent cellular

encapsulation and clogging. Piezoelectric inkjet printing uses the same technique except in lieu of using impulse heat, an impulse voltage is applied to a piezoelectric crystal inside the head which then vibrates and sends shockwaves through the reservoir. These shockwaves created by the crystal causes material expulsion. The valvular method uses a constant pressure that impulses open and shut very rapidly. The benefits to this method are the resolution, and low cost. Where this method struggles is that it requires relatively low viscosity bioink (<10 CP) where high viscosity liquids cannot be effectively dispensed. As a result, the mechanical strengths of these structures are weaker. Thus, this method fails to provide sufficient strength to these structures.

Laser assisted bioprinting (LAB) can be executed in two different ways. The first method requires the deposition of fine particles of a material one layer at a time, after which a laser melts and fuses the top layer to the one below it in a pattern forming a solid piece inside the fine particulate that then needs to be removed from the finished product (**Fig 5**).

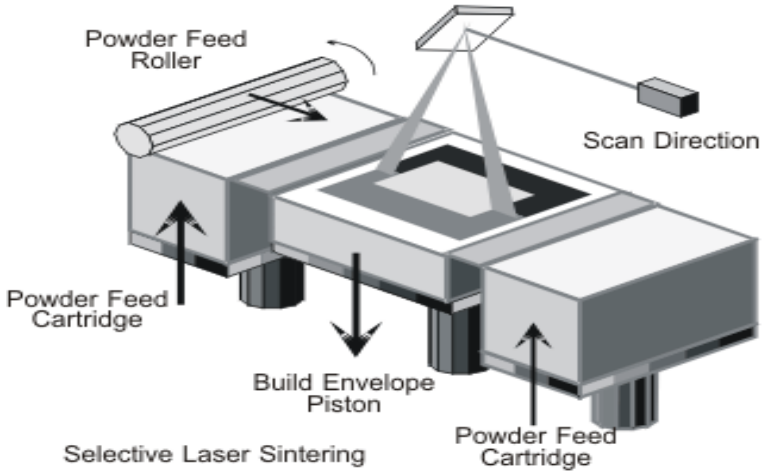

Figure 5: *This diagram shows the deposition sintering method of laser based printing (Bakhshinejad, Ali, and Roshan M. D'Souza. "A Brief Comparison between Available Bio-printing Methods.")*

A similar procedure can be executed by using a sacrificial material and a laser to generate force to expectorate spheroids of cells onto a substrate. This method is also a form of laser assisted bioprinting (**Fig 6**).

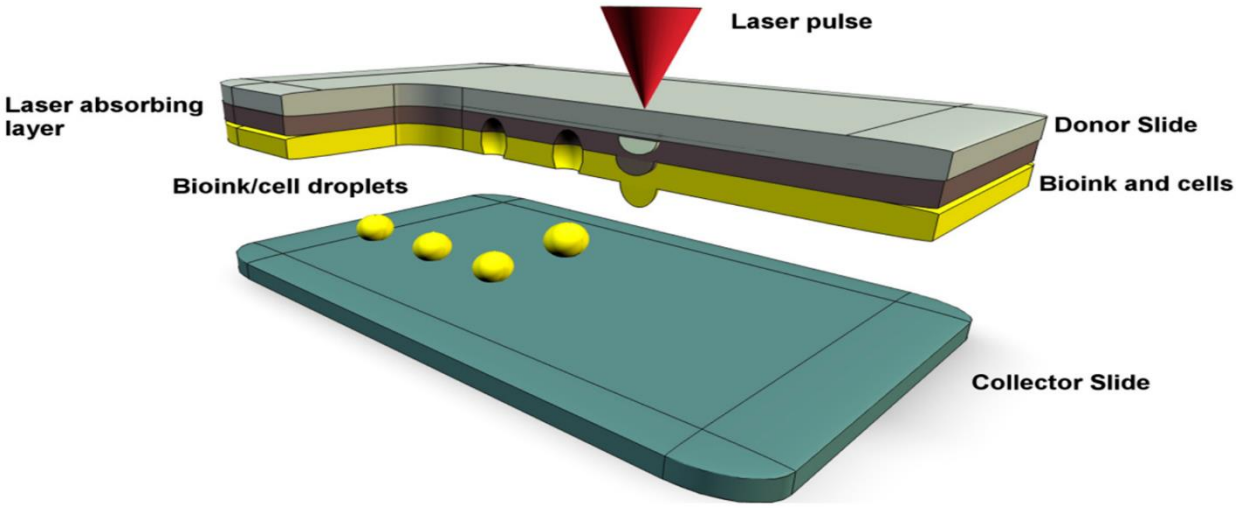

Figure 6: *Schematic of laser assisted printing done using a sacrificial ribbon coated with cells on the underside (Bakhshinejad, Ali, and Roshan M. D'Souza. "A Brief Comparison between Available Bio-printing Methods.")*

This technique involves the use of a donor strip of material (ribbon) that is covered on one side with biomaterials and the other side with absorptive materials, in this way as the laser hits the ribbon the excitation causes the material to be donated onto the substrate beneath it. This method has poor deposition rate (as it's mostly in nanodroplets), and the mechanical stability of printed constructs is very poor. Also, there is no way to create internal vasculature.

Each printing method can be modified for bioprinting, the limiting factors for each method being what kinds of inks/materials are viable, and the ease of modification of each method for biomaterials. For SLA printing for example, an ink could be used that crosslinked in ultraviolet light (gelatin methacrylate, polyethylene diacrylate, etc.), however the ink used would have the requisite of also being oxygen inhibitive to the crosslinking process because the mirror

directing the light beneath the bath does not have a very fine focus. This chemical prerequisite for using this technique is very limiting in the materials available.

Fused Laser Sintering is one of the most versatile forms of 3D printing in general because they have the widest range of viable materials without modification specifically; polymers (natural and synthetic), ceramics, and metals. Modifying this method would require a great deal of effort and work. For starters, a water-tight build volume with an accurate method to disperse bioink in lieu of powdered material. The laser used to melt the material would also need to be changed with one that could crosslink UV crosslinkable inks without killing cells. The ink that would be most applicable for this process would be GelMa or PegDa. A drawback and the reason this method was not selected even though it has such a wide variety of material applications, is twofold. Primarily, the quality of prints using this method results in a very porous structure, and requires a very fine and consistent size of powdered material to maintain consistency. Secondly, creating large baths of cells and uncrosslinked hydrogels, with a photo-initiator, causes necrosis in the cells due to the cytotoxicity by the photo-initiator.

SLA printing has the benefit of making solid objects without layers, meaning that bulk structures could be created without structurally sound materials or sacrificial materials. Stereolithographic printing has the downside of needing to use very specific photoreactive oxygen inhibitive materials, that are at the same time cytotoxic making it rather restrictive for available materials in tissue engineering and cell viability. SLA printing is closely connected with laser assisted methods, and as such has limited scalability.

FLS printing also has merit in biological modification, as a simple modification to the laser could allow it to crosslink polymers instead of melting metal and plastic, however, the

downside with this method is that it is not robust enough to modify any further to any other type of material.

FDM printing is nearly ideal for modification of 3D printers to bioprinters as the technique is so robust, and modifications can be made multiple ways to accomplish slightly different tasks, as we did here. FDM printers work by melting material in the head and extruding the liquid while the head moves in the XY plane and the material re-solidifies. This allows the next Z layer to be printed on top of the one printed before it. This layer method can be used to satisfy all prerequisites for tissue engineering as well as resolve some of the difficulties that are seen.

Each additive manufacturing method was taken into consideration for bio-fabrication, however, the FDM printing process was the most favorable due to its speed, cell viability, and *availability of materials (**Table 1**).*

Category	Inkjet	Microextrusion	Laser printing
Material viscosity (mPa/s)	Low (3–12)	High ($30–6\times10^7$)	1–300
Gelation/cross-linking methods	Chemical or photo-cross-linking, temperature	Chemical or photo-cross-linking, temperature	Chemical or photo-cross-linking
Print speed	1–10,000 droplets/s	10–50 μm/s	200–1600 mm/s
Resolution	50–300 μm wide droplets	100 μm to 1 mm wide	50 μm
Accuracy	Medium	Medium–low	High
Cell viability	>85%	40%–80%	>85%
Cell density	$10^6–10^7$ cells/mL	High: cell spheroids	$10^6–10^7$ cells/mL
Biomaterials used	Hydrogels, fibrin, agar, collagen, alginate	Hyaluronic acid, gelatin, alginate, collagen, fibrin	Hydrogels, nano-hydroxyapatite
Mechanical/structural integrity	Low	High	Low
Fabrication time	Medium	Short	Long
Scalability	Yes	Yes	Limited
Cost	Low	Medium	High
Example applications	Skin,[22,53] vascular,[65,66,69] cartilage[46,78,79]	Trachea,[38,71] cardiac valve[75–77]	Skin[54,55]

Table 1: *A direct comparison of various printing methods and quantitative outcomes. The FDM (micro extrusion) method was chosen because it has the highest variety in usable materials, maintains cell viability, and is very fast.*

Fused Deposition Manufacturing allowed for a greater degree of freedom and customizability with usable materials, including thermoplastics as well as soft materials and cells. FDM printing is a very simple, robust technique, making it ideal for modification and use

beyond its original intent. The challenge presented by using FDM printing is that creating large 3D constructs with bulk thickness without the use of sacrificial materials can be difficult for soft biomaterials that do not have a great deal of structural integrity. This method was chosen because its strengths matched what we wanted to accomplish, and its weaknesses were acceptable within the context of our goals. This isn't to say that this is the best method overall, but that the weaknesses it presents towards potential cell viability, fidelity, and integrity; could be reduced or there could be means to work around such shortcomings.

The aim of this thesis is to expand the utility of off-the-shelf 3D printers for work towards biomaterials, hydrogels, and cells; in order to apply the benefits of additive manufacturing to the world of tissue engineering and biological research. The rise in popularity of 3D printers has made them much cheaper and easier to access; therefore, they are easier to modify for use beyond their original function. The purpose in applying 3D printers to biological research is that the printers can create user defined geometries out of biomaterials with a high degree of accuracy and precision that can be replicated exactly. The main advantage here is that the geometries are user defined, but can be repeated with exact precision. The critical quantification for these off the shelf printers is whether they are capable of functioning as bioprinters, and if so what sort of capabilities do they have as such. To answer such a question requires a comprehensive understanding of extrusion mechanics, 3D printing techniques, and a wealth of knowledge in tissue engineering and cell culture.

1.2 FDM Printing

Thermoplastics are the most available materials for FDM style printers, with polylactic acid (PLA), or acrylonitrile butadiene styrene (ABS) being the two most widely used materials. These are the most common thermoplastics used because of their relative strength and ease of

extrusion. There are other materials that can be used by FDM printers and there is a constantly expanding array of materials with the only limiting factor being materials that can be formed into a filament, and fed into the machines in a controlled manner. A large portion of this project was conducted with the original head on the printer while custom materials were created for various biological applications.

The first place to start in augmenting the utility of off the shelf printers was to make custom materials that could fulfill certain needs in our biological applications before modifying the entire print-head to work with cells and hydrogels. In doing this we could increase the functionality without altering the process flow of the printing method. The advantage of creating biocompatible thermoplastics to 3D print was that it uses the same system without any need for hardware modification, and only slight software modification. The disadvantage being that we were using materials that hadn't been printed before and therefore required a good deal of experimentation for consistent operation, and later, validation. The utility added by printing biopolymers is in osteogenic tissue engineering endeavors that require unique geometries.

The goal, with regards to the materials used by the printers was to expand the types of materials and various properties both chemical and physical of said materials so that we could develop said material and strategy to fabricate it using a standard FDM printer. The array of materials ranges from shape memory polymers (SMPs), naturally occurring polymers, synthetic polymers, and various composite materials.

1.3 Cell Culture and Tissue Engineering

The point of cell culture techniques is to observe and manipulate the behavior of cells in a laboratory environment. The shortcoming here is that a large portion of cellular behavior is dependent on the environment of the cell and its relation to other cells around it. The easiest way

around this problem is to study tissue samples as a whole; however, tissue samples tend to not survive very long in vitro, therefore a solution proposed would be to create an environment that simulates in vivo stimulus in vitro.

Culturing cells in 3D space allows researchers to study how cells grow in all directions, and how they would react to intracellular signaling as they would in vivo. Current cell culturing methods study cells that are either adherent to the bottom of a petri dish or for some cells in fluid suspension, but both methods are incapable of simulating in vivo situations that can be created by 3D constructs.

The problem we were faced with was whether it was possible to make a commercially available FDM 3D printer capable of using bio-compatible materials and cell laden inks without spending exorbitant amounts of money and resources. Furthermore, was it possible to do so in such a way that any person could do the same thing with any commercially available FDM 3D printer. This question covers the entire scope of our work, and what was done with these printers, with the ultimate goal being to print living cells that would grow into tissues, and in future work, organs.

Typically, in cell culture the cells are grown in the bottom of a wide flask or suspended in solution depending on cell type and what they are needed for. The media in which cells are maintained supplies all the nutrients, growth factors and required gases for the cells. The greatest benefit to this method of studying cells is that it allows for complete control and automation over the physiochemical environment that the cells are in at any given moment in time. The physiochemical environment consists of the pH, temperature, dissolved gas concentration, and hormones. The level of control over the cellular environment is the single greatest benefit that cell culture techniques have. It is important to understand these benefits to ensure that we

maintain them when we move toward tissue cultures, and printing methods to create them. The primary disadvantages to cell culture are that they are costly, that maintaining aseptic environments can be difficult, and for each specific cell type a different expertise is needed to ensure optimal cell growth. Experimentally the primary challenge is that since the cells grow so rapidly in an artificial environment, there can be genetic heterogeneity in the population making some results difficult to interpolate.

The goal behind this project is to mitigate the shortcomings in tissue and cell cultures by using FDM additive manufacturing techniques, however to do so we must first expand the utility of classical 3D printers. This paper details that journey.

Chapter 2: Custom Thermoplastic Extrusions for Fused Deposition Modeling 3D Printing

2.1 Introduction

Bone has emerged as the second most transplanted tissue in the world as a result of patient traumas, aging populations, osteoporosis, and the prevalence of bone tumors.[1] Since current clinical therapies have not been sufficiently successful, the field of bone tissue engineering continues to develop new bone substitutes by combining porous biomaterial scaffolds with relevant cells and growth factors. Important aspects of bone tissue engineering include the fabrication of porous polymer scaffolds with patient-specific geometries, the necessary structural strength to house living cells, and the ability to facilitate tissue in-growth during *in vitro* development of bone tissue or during *in vivo* implantation.[2-6]

To promote cell proliferation, tissue growth, and remodeling, porous scaffolds have been developed using several different manufacturing approaches. Use of traditional fabrication methods such as solvent casting, freeze drying, porogen leaching, fiber bonding, dual phase separation, and gas foaming, typically create simple geometries and only allow limited control over pore-interconnectivity within 3D scaffolds, both of which are extremely essential for bone tissue applications.[7-9] With the goal of developing scaffolds with a 100% pore-interconnectivity, additive manufacturing and other Solid freeform fabrication (SFF) techniques such as laser sintering [10], stereolithography [11], and Fused Deposition Modeling (FDM) [3, 12] have been used.[5, 6] Several researchers have developed manufacturing equipment based on FDM principles where a polymer spool is extruded through a heated nozzle and can subsequently be moved using commands obtained from a computer aided manufacturing program.[12, 13]

While most labs have typically developed custom made extrusion-based equipment to print user-defined 3D scaffolds, the emergence of easy-to-use commercial 3D printers has allowed other researchers with non-manufacturing backgrounds to print complex 3D models. For example, physicians and clinicians use MakerBot printers to develop anatomically accurate physical models for educational purposes and to practice surgeries on physical models. The drawback, however, is that these physical models can only be built using commercially available and easy-to-use polymer spools. Biomaterial spools such as polycaprolactone (PCL), a thermoplastic commonly used for bone tissue engineering applications, [14] are not commercially available, and have to be custom-made in research labs. These direct-writing techniques that rely on the properties of colloidal biomaterial inks are able to be used to either print droplets, hot-melts or continuous filament printing techniques, [15-19] but need specialized manufacturing knowledge to operate. Furthermore, incorporation of living cells within 3D printed scaffolds is yet another significant challenge as cells seeded on scaffolds with small pore-sizes typically results in uneven cellular distribution throughout the scaffold, with most cells adhering to the periphery of the scaffold.

In this work, we demonstrate the synthesis and fabrication of 3D scaffolds using hybrid polycaprolactone (PCL) spools and an easy-to-use commercial *Makerbot* 3D printer. Hybrid spools were developed by mixing fillers such as poly-L-lactic-acid (PLA) or hydroxyapatite (HA) particles within the PCL matrix, and followed by characterizing mechanical and materials properties. We also demonstrate the incorporation of living cells into the interior of the log-pile scaffold with a facile and easy-to-use technique.

2.2 Materials and Methods

2.2.1 Development of Hybrid Spools

Spools were made using a Randcastle microfilament extruder (Randcastle Inc.) and a base material of polycaprolactone (PCL) pellets having a 3mm diameter and 70kDa-90kDa molecular weight (Sigma Aldrich) **(Fig. 7).**

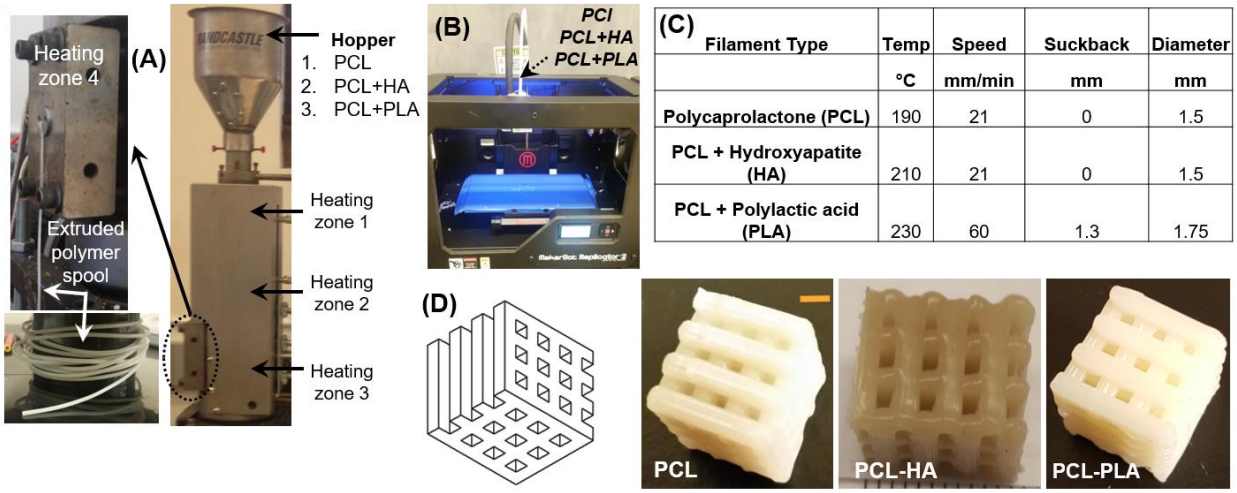

(C) Filament Type	Temp	Speed	Suckback	Diameter
	°C	mm/min	mm	mm
Polycaprolactone (PCL)	190	21	0	1.5
PCL + Hydroxyapatite (HA)	210	21	0	1.5
PCL + Polylactic acid (PLA)	230	60	1.3	1.75

Figure 7: *(A) The raw material is fed into the filament extruder creating a long strand of three polymer spools (PCL, PCL-HA and PCL-PLA). (B) commercially available MakerBot Replicator 3D Printer. (C) The printer settings are set for each filament spool respectively. (D) The model of the log-pile scaffolds and the printed counterparts to the right. Scale bar: 2mm. 234x95mm (300 x 300 DPI).*

The raw PCL material and the fillers, either hydroxyapatite (HA) (Sigma Aldrich) or poly-L-lactic-acid (PLA) were mixed and fed into the extruder's hopper. The shear force of the machine's extrusion screw fed the raw material (PCL) and filler (either PLA or HA) into four heating zones, allowing for homogenization of PCL-PLA composites and mixing of PCL-HA composites. A cooling zone was located below the third heating zone and the thread of the screw was reversed, thereby causing a buildup of pressure that forced the melted polymer mixture out of the head (heating zone 4). The temperatures were kept at 160° Fahrenheit (72° Celsius), which is above the melting point for PCL (140° Fahrenheit [60° Celsius]), and would keep the pure PCL polymer in a liquid state during the extrusion process, while maintaining constant pressure.

For the PCL-HA spool the temperatures were raised to 170°F (76.6°C) to allow HA powder to mix with liquid PCL, and for the PCL-PLA spool the temperatures were raised to 320°F (160°C) to melt both of the polymers since PLA has a melting point between 300°-320°F. The pressure for each spool was kept at 1000 psi +/- 200 psi and fed through a custom nozzle with an opening diameter of 1.57mm. The filament expanded once it left the extruder head to the appropriate 1.75±.05mm so that it could be wound into spools and fed into the commercially available 3D printer, *MakerBot Replicator 2* (*MakerBot Industries*) **(Fig.7B).**

2.2.2 Chemical Composition and Testing

To determine the final material composition post extrusion and printing, a high resolution thermogravimetric analysis (TGA) was performed on PCL, PCL-HA and PCL-PLA samples using a Q500 thermogravimetric analysis (TA Instruments). The samples were heated to and beyond their degradation points while being weighted so the amount of each polymer/component could be determined based on weight percentages.

2.2.3 3D Printing and Mechanical Testing

Spools were loaded into the *MakerBot* and several different software were used to generate the .stl files used to make the g-code for the log-pile scaffolds. *Solidworks* (*Dassault Systems*) was used to make the log-pile geometry with two different sizes: (1) 10.5mm x 10.5mm x 12mm, and (2) $6mm^3$, with sufficient porosity to obtain repeatability and mechanical reliability. In addition to log-pile scaffolds, two complex geometries were fabricated using a computer tomography (CT) scan of a right femur. An .stl file was downloaded from *thingiverse.com,* and subsequently added to *Meshmixer* (*Autodesk*), a program that allows for

unique customization of .stl's to use different mesh generating tools in order to make user-specified designs.

To test the mechanical strength of the scaffolds, the larger log-pile structures **(Fig. 7)** were placed between two plates on a compression MTS machine (Sintech 2G) with a 10K newton load cell. The samples were compressed to failure and the machine recorded the downward cross head travel and the force from the load cell.

2.2.4 Cell Incorporation within Log-Pile Scaffolds

A mixture of gelatin methacrylate (GelMA) mixed with human osteosarcoma cells (Saos-2) were incorporated within log-pile scaffolds. Using a previously reported protocol [20, 21] GelMA was synthesized. Briefly, porcine skin gelatin was mixed at 10% (w/v) in phosphate buffered saline (PBS, *Thermo Fisher Scientific*), stirred at 45ºC, and methacrylic anhydride added to the solution and stirred for 3 hours. After stirring, the solution was dialyzed against distilled water for one week (40˚C), freeze-dried, and stored at -80°C until needed. For cell encapsulation experiments, a final GelMA prepolymer solution of 7% was prepared by mixing freeze-dried GelMA with PBS and .25% *UV photo-initiator Irgacure 2959* (*Specialty Chemicals*, Switzerland) at room temperature.

Human osteosarcoma cells (Saos-2) were purchased from *American Type Culture Collection* (ATCC) and cultured in *Dulbecco's Modification of Eagle's Media (DMEM*; *Life Technologies*) supplemented with 9% fetal bovine serum (v/v) *(FBS lot K14133; Atlanta Biological*), 1% penicillin-streptomycin *(Life Technologies*) and 1% GlutaMAX (*Life Technologies*). Cells were passaged using .25% trypsin-EDTA *(Life Technologies*) and maintained at 37°C. A mixture of GelMA and Saos-2 cells was created by adding 20μL of a cell solution containing approximately 5000 cells/μL to 130μL of GelMA prepolymer solution.

Cell/GelMA solution was pipetted dropwise onto sterilized PCL, PCL/PLA, and PCL/HA scaffolds and subsequently crosslinked using a *Hamamatsu LED Controller (Hamamatsu C11924-511; Hamamatsu Photonics K.K., Japan*). Viability of cells were analyzed using a Live/Dead assay on day 5. To evaluate cell viability, scaffolds were placed in media containing 1:2000 dilution calcein-AM (*Life Technologies*) and 1:500 dilution ethidium homodimer *(Life Technologies*) and incubated at 37°C for 1 hour. After 1 hour, scaffolds were cut into three equal pieces using single edge industrial razor blades and imaged using an epifluorescence microscope (*Nikon, Eclipse E-400, Nikon Corporation, Japan*). Raw .tiff images were taken for all samples and processed linearly for contrast and brightness using *Adobe Photoshop CC 2015 (Adobe Systems Inc., CA*). Processed images were overlaid and false colored to create final live/dead images with green representing live cells and red representing dead cells. Brightfield images were not processed linearly for contrast and brightness. Images were also obtained using *Hirox KH-8700* digital microscope (*Hirox-USA, Inc., NJ*).

2.3 Results

2.3.1 3D printing using hybrid PCL spools

The overall process of manufacturing log-pile geometries using hybrid spools is depicted in Figure 7. To manufacture spools, a *Randcastle* microfilament extruder was used to combine base PCL material with either HA or PLA **(Fig 7A)**. Extruded filaments of an appropriate diameter of 1.75±.05mm could then be wound and fed into a commercially available *Makerbot Replicator 2* 3D printer (**Fig.7B**).

A range of process parameters used for 3D printing (**Fig.7C**) were determined from the melting point and degradation point information for each spool that were obtained from thermogravimetric analysis. A set of temperatures were chosen within these ranges and

optimized such that the spools could be fed into the machine in a reliable and repeatable manner. Temperature, which was the critical variable, was adjusted to allow easy printability (extrusion) using viscous melts.

For clarity, the "diameter" variable does not refer to the diameter of the spool, but rather to a number fed into *Makerbot* Slicer program. This was necessary to compensate the pushing force on various spools. For PCL and PCL-HA spools, this variable was decreased from 1.75mm (standard size) to 1.5mm to force the extruder to push more filament out, effectively compensating for the differences in density from PLA (1.4g/cm^3) to PCL (1.14g/cm^3). Finalized log-pile prints were realized after optimizing the printing conditions (**Fig.7D**).

2.3.2 Composition and mechanical properties of printed scaffolds

High-resolution thermogravimetric analysis **(Fig. 8A)** was used to quantify the exact amount of filler (PLA or HA) in the PCL matrix.

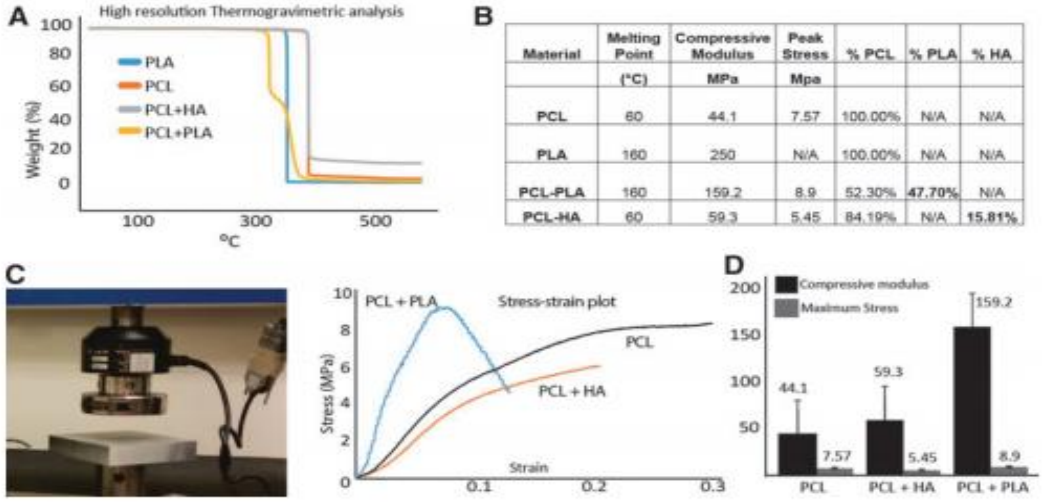

Material	Melting Point	Compressive Modulus	Peak Stress	% PCL	% PLA	% HA
	(°C)	MPa	Mpa			
PCL	60	44.1	7.57	100.00%	N/A	N/A
PLA	160	250	N/A	100.00%	N/A	N/A
PCL-PLA	160	159.2	8.9	52.30%	47.70%	N/A
PCL-HA	60	59.3	5.45	84.19%	N/A	15.81%

Figure 8: (A) High-Resolution TGA of Polymer spools. (B) Results in tabular form showing the degradation points and percentages for each compound. (C) Compression testing apparatus to obtain mechanical properties of log-pile scaffolds. (D) Stress-strain plots and bar graphs of modulus and maximum stresses for each polymer spool. TGA, thermogravimetric analysis.

The sample was heated above its degradation point and the derivative of the heat of the furnace (the rate of heating) was measured as it related to the drop-in weight of the test-sample. This analysis was used primarily to demonstrate two distinct degradation points and a % composition of hybrid samples (**Fig. 8A, B**). Both PCL and PCL-HA had a degradation point of 383°C and the change weight between PCL and PCL-HA (15.81%) was representative of the weight of HA present in PCL-HA spool, as inorganic HA does not degrade and remains on the balance after complete degradation of the PCL component. The actual amount of HA was found to be slightly lower after thermogravimetric analysis than was present during the spool-making process (20%).

Similarly, the amount of PLA was found to be slightly lower after analysis. The mixture of PCL and PLA had two distinct degradation points (the first degradation point for PLA being at 325°C and the second point for PCL being at 355°C) which were used as markers for determining the percentage of each constituent in the combined spool (**Fig. 8B**). From the thermogravimetric analysis, the exact amount of PLA in PCL matrix was determined to be 47.7%, a minor deviation from the 50:50 ratio initially put into the extrusion hopper

Mechanical properties for log-pile scaffolds were obtained from the stress-strain curves using a standard MTS machine **(Fig. 8B, C, D)**. PCL-PLA, PCL-HA and PCL had compressive moduli of 159.2 MPa, 59.3 MPa and 44.3 MPa respectively. The increase in moduli in the hybrid PCL-PLA spools was a result of the higher moduli of pure PLA (250 MPa) filler added to the PCL matrix.

2.3.3 3D Printing of Complex Porous Geometries

PCL is a premier biopolymer used for bone tissue engineering applications and its ability to be readily augmented and printed in specific shapes via commercial 3D printers could lead to

enhanced clinical solutions for bone defects. Custom scaffolds for bone repair can be printed from Cartesian data obtained from a CT scan, allowing the possibility of patient-specific support

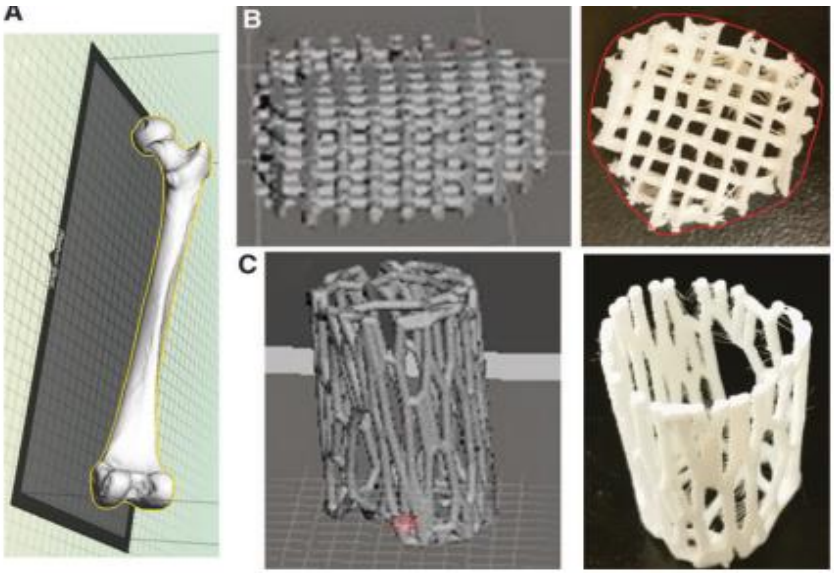

cages for bone tissue engineering (**Fig. 9**.)

Figure 9*: (A) Cartesian data for a human femur were into the MakerBot Desktop. (B) A slice from the diaphysis of the femur was taken and Lattice meshed in Meshmixer. On the right is the 3D printed model in PCL. (C) Longer slice from the diaphysis was Voronoi meshed in Meshmixer to create a hollow cage-like representation of the outside of the femur. On the right is the 3D printed PCL model.*

The first geometry shown was created in order to have a log-pile lattice similar to the log-pile geometry described earlier, but modified with macro-scales and boundaries derived from the .stl file of a human femur **(Fig. 9A)**. A scaled femur model was placed into the mesh program and sliced to obtain a small cross section of the diaphysis. The *Meshmixer* program was then used to render the model into various layers while keeping the same external geometry (**Fig. 9B**, red outline). The lattice structure was used to maximize the internal free-space while minimizing the amount of material used to support reliable printing of the structure.

To increase the internal free-space, another type of scaffold was developed using Voronoi analysis, a solution which only uses the surface data in the .stl file (**Fig. 9C**). The Voronoi was made by reducing the number of triangles on the surface of the .stl file and subsequently using

the Dual Edges function to give them all a tubular thickness and density. For each filament, the .stl's were uploaded into the *Makerbot* Desktop software and the settings were edited in the slicing program to obtain printing repeatability. The resulting hollow cages maintained the external geometry as derived from the CT scan, while still leaving space for the incorporation of biomaterials containing living cells.

2.3.4 Cell incorporation within log-pile scaffold

To visually model a process in which live cells could be contained within a 3D printed log-pile structure, a 6mm^3 PCL log-pile scaffold was placed inside a rectangular chamber and subsequently covered with 7% GelMA containing 15% (v/v) MiO orange coloring (*Kraft Foods Inc*., IL) (**Fig. 10A**).

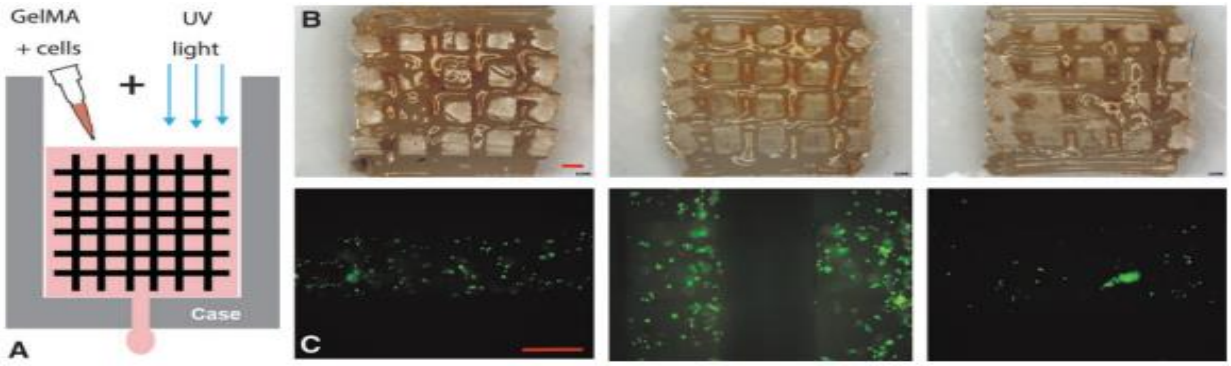

Figure 10: *(A) Schematic representation of the process used for incorporating living cells within printed scaffolds. Case was slightly larger than 6 mm^3 log-pile structure to allow for GelMA-cell solution perfusion. (B) PCL scaffold infused with 7% GelMA containing 15% (v/v) MiO orange coloring to show complete perfusion of GelMA throughout scaffold (left to right: PCL GelMA top, PCL GelMA middle, PCL gelMA bottom). (C) Live(Green)/Dead(Red) calcein-AM/ethidium homodimer pictures from PCL/PLA scaffold (left to right: PCL-PLA GelMA top, PCL-PLA GelMA middle, PCL-PLA GelMA bottom). GelMA, gelatin methacrylate.*

The GelMA was pipetted drop-wise onto the PCL scaffolds and simultaneously solidified using UV light exposure. Sliced sections from the top, middle, and bottom areas successfully showed a thorough incorporation of GelMA within in the interiors of the log-pile scaffold **(Fig. 10B)**. As reported, the infusion process was facilitated by using a plastic column containing a

small outlet port in the bottom of the chamber, thereby allowing an even flow-through of GelMA solution throughout the entire scaffold.

For cell encapsulation, a mixture of gelatin methacrylate (7% GelMA) and human osteosarcoma cells (Saos-2, 5000 cells/μL) were incorporated within a PCL-PLA log-pile structure in a similar manner. After 5 days, the log-pile structure was incubated with calcein-AM and ethidium homodimer and imaged fluorescently for live/dead analysis **(Fig. 10C)**. Live cells (green) were shown prevalently in the top, middle and bottom sections of the sliced log-pile scaffold. Similar results were obtained for PCL and PCL-HA log-pile scaffolds (results not shown here).

2.4 Discussion

We choose PCL as our base material due to its extensive use in developing scaffolds for bone tissue engineering. PCL is a semi-crystalline aliphatic polymer with suitable rheological properties such as glass transition temperature and melting point, and is readily biodegradable by hydrolysis [22]. HA, while a major component of native bone that has been shown to promote bone mineralization, is difficult to process due to its brittle characteristics [23, 24].

One significant challenge in creating the composite spools was the difficulty in achieving filaments of consistent diameter (1.75mm), a necessary requirement for several commercially available 3D printers. This aim was achieved by controlling the extruder-pressure and barrel screw revolution, and by varying the "suck-back" variable on the *MakerBot* (**Fig. 7C**). The "suck-back" is typically set at 1.3mm at a velocity of 25mm/s to break off each extrusion. Since PCL has a high specific heat, "suck-back" was set to zero to avoid blocking the printer nozzle.

A second challenge that will need to be addressed in subsequent studies is the apparent loss of both HA and PLA in the spool manufacturing process (**Fig. 8B**). As previously

mentioned, there was a slight decrease in the amount of HA and PLA measured in the composite PCL-HA and PCL-PLA spools as compared to the starting materials placed into the hopper. While the exact cause of the loss is unknown, it can most likely be attributed to the adhesion of HA and PLA to either the inner barrel of the extruder or any of the other various surfaces that they would touch throughout the manufacturing steps.

Natural bone is an organic/inorganic composite typically consisting of cortical and cancellous bone [25] with a compressive modulus of 131-224MPa and 5-10MPa respectively. As reported here, the compressive results with the hybrid spools had moduli ranging 59-159MPa, thereby falling well within the target zone required for bone tissue engineering. These results, in conjunction with the generation of a custom scaffold from CT scan data, brings credibility to the long-term goal of developing patient-specific support cages for bone tissue engineering.

Model scaffolds used for bone tissue engineering should mimic both the mechanical and chemical composition of natural bone. Since natural bone contains organic collagen fibers [25], we decided to incorporate GelMA laden with living cells into printed log-pile scaffolds. We chose GelMA, a denatured form of collagen, as the model hydrogel because it contains an abundance of biologically active cell-binding sites, has highly controllable mechanical properties, and provides increased transparency for imaging. Human osteosarcoma cells were chosen in this study as they are a robust cell line commonly used in the initial stages of new bone defect models. By choosing osteosarcomas for our initial work, we limited donor dependent differences that would arise from primary cell lineages. In the future, we plan to use bone marrow derived stem cells to obtain an understanding of how scaffold design parameters influence the cell number and their metabolic activities. Integration of the structural cage with cell-laden GelMA showed a construct compatible with the multifunctional nature of bone, and

showcased the potential for a tissue engineering model capable of improving the handling characteristics of soft hydrogel constructs under weight bearing conditions. The open-frame design provided sufficient space for cell-laden hydrogels to support bone mineralization, remodeling, and integration with host tissues; while at the same time providing a stabilizing interface between engineered and host tissues.

2.5 Conclusion

Polymers, with their favorable processing properties, have been extensively used to develop 3D scaffolds for tissue engineering applications. 3D printing of tissue engineering scaffolds often requires customized instruments such as heated extruders and computer controlled XYZ stages with precisely coordinated movements to lend themselves properly in the creation of biopolymer properties (viscosity, melting temperature, printing speed). This project developed hybrid spools with FDA approved PCL polymer as the base material as well as hybrid spools readily compatible with commercial 3D printers such as the *MakerBot.* Porous geometries were printed using CT-scan data with both internal log-pile lattice structures as well as external meshed structures. Finally, we demonstrated that living cells mixed in gelatin hydrogels could be incorporated within the log-pile scaffolds with high cellular viability.

Chapter 3: Modifications to Bath Based 3D printing Method for Printing Soft Biomaterials

3.1 Overview of bath technique

A Bath based printing method uses a sacrificial material in which to inject uncross-linked hydrogel. Using the chemical interactions between the ink and bath material this causes physical crosslinking. With the use of commercial 3D printing, this technique can be used to accurately deposit hydrogels in a given volume in custom geometries. The entire technique can be visualized with the following flow diagram (**fig 11**).

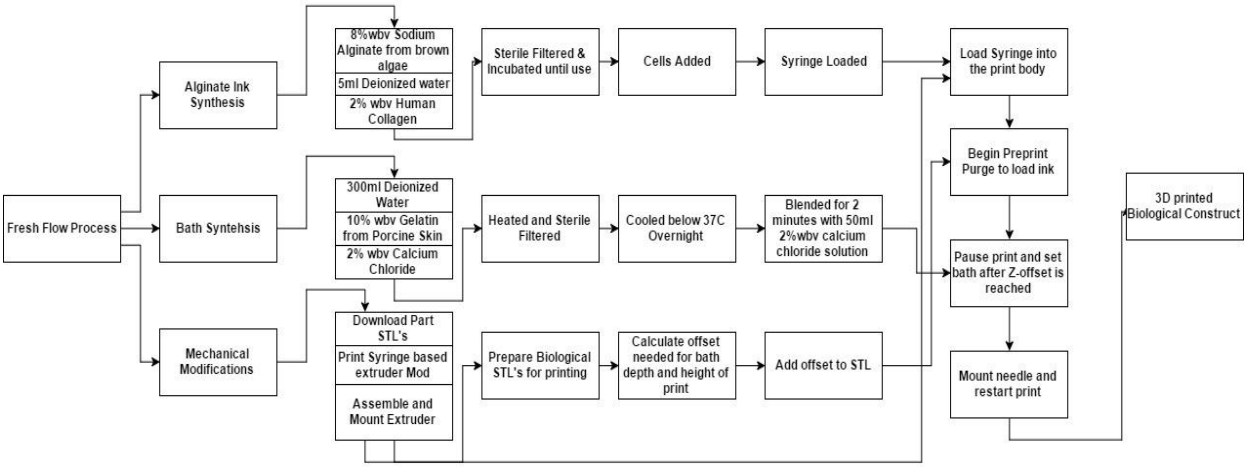

Figure 11: Process flow chart for bath based 3D printing. This method consists of 3 parallel processes happening concurrently.

Bath based printing is a technique used to print biomaterial into a bath of emulsified gelatin. It stands for freeform reversible embedding of suspended hydrogels, and is a technique created by Adam Feinberg at Carnegie Mellon University, as a method of 3D printing complex biological structures using sodium alginate and a suspension bath as a support material.

Sodium alginate is a biologically derived polysaccharide based polymer that normally acts as a thickening agent (thixatrope), and physically cross links in the presence of calcium cations. This crosslinking process is inert to cells making it ideal for printing cellular constructs out of hydrogels. It works by using an alginate solution to hold cells in suspension while an emulsion of gelatin and calcium chloride acts as a support material. The presence of calcium ions, cross links the alginate by reacting with the sodium causing the long polymers to form egg crate shapes that entangle and trap cells.

The gel bath supports overhanging materials that would normally be printed without support and therefore fail, this is a massive advantage in printing biologically derived constructs as most prints require support material due to complex 3D geometry. Once the solution is reacted with the calcium ions it becomes a solid embedded in the support material, the strength of which is dependent on the amount of alginate in the ink solution (by volume). The ingenuity of this method is that support material can then be melted away simply by heating the bath to 37°C (body temperature) thus releasing the printed construct from the bath. The bath technique was created as a means to turn *MakerBot* 3D printers into Bioprinters, and make it easier for labs to create bio-scaffolds and tissue precursors without substantial financial investment.

Our goal was to take the process developed by Professor Feinberg, refine it, and optimize it. To make it more efficient and robust by adding and modifying parts and procedures during the process. To make the system more reliable and easier to use with little technical knowledge needed to create and operate the machine modifications.

3.2 Materials & Methods

This entire phase of the project was conducted using a *MakerBot Replicator 2*, a set of 3D printed parts to create the extruder modification, acme screws and nuts, as well as delrin

spacers accurately machined to make the machine operate more concentrically. Sodium alginate, human collagen, and gelatin were used to create the ink. Bath based printing is dependent on the 3D printer modifications that were modified (**fig 12**).

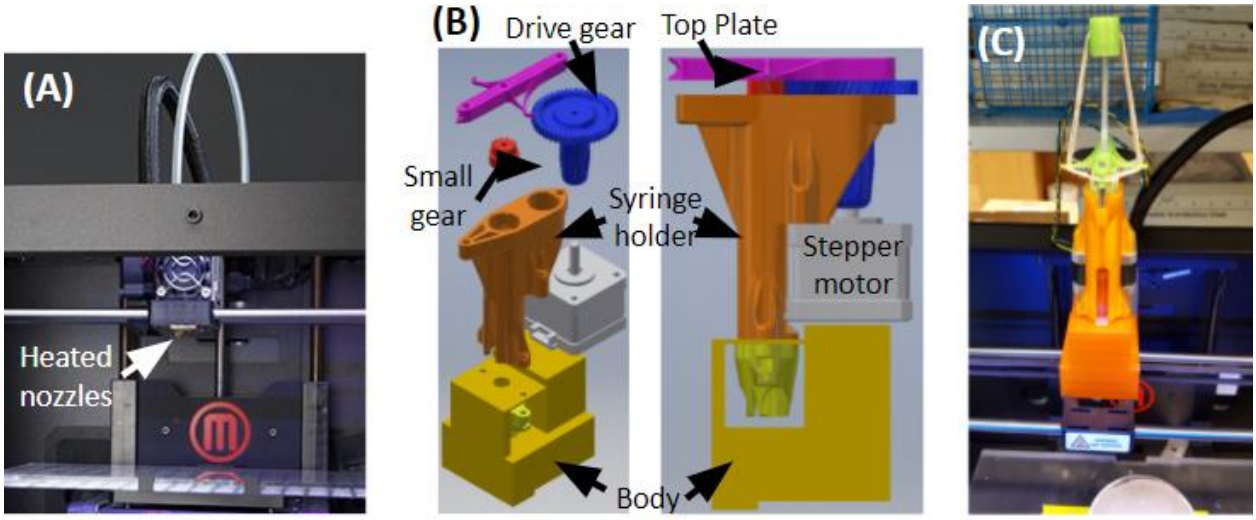

Figure 12: *The set of 3D printed parts that were printed, and then mounted on the 3D printer to create the bath based modifications.*

3.2.1 Preparations

The process of bath based printing procedure is as follows (all %'s are in weight by volume). The solutions are prepared, one from alginate and collagen (8% NaAlg and 2% collagen), the other from gelatin and calcium chloride (10%, and 2% respectively). Next the gelatin and alginate solutions are both vacuum filtered to ensure sterility. Once the two solutions are sterile, the alginate solution is left in an incubator while the gelatin solution is left in a sterile refrigerator for 12 hours.

Once the gelatin solution solidifies, it is then emulsified in an *Oster* kitchen blender for 2 minutes. Multiple attempts were made to create the emulsion, with 2 minutes being optimal for particle size and overall. Any shorter and particle size and consistency became an issue, though going longer wasn't found to have a great impact on performance. At around the 3-minute mark

the viscosity of the mixture appeared to drop, and no longer exhibited the unique shear properties required to be a support bath and was more like a thick liquid, not a Bingham plastic.

3.2.2 Replistruder mounting:

Cad models are printed using a *Replicator 2*, these models can then be assembled into a working version of the replistruder. Once the parts have been printed and assembled, the head on a *MakerBot Replicator 2* or 2x can be unmounted, the feed motor in the back removed and mounted to the drive gear of the replistruder. The entire assembly can then replace the conventional head on the 3D printer. A mount can be provided by the original creators of the replistruder, however, we chose to forgo this option in favor of a custom design to allow us to better set our offsets.

The custom mount allows for the replistruder to be directly mounted onto the carriage of the printer itself. A syringe containing the bio-ink of choice must first be loaded into the main body of the replistruder prior to mounting it to the carriage. Once the syringe is loaded the entire assembly is then mounted and the drive gear turned by hand until the acme screw touches the top of the syringe, this eliminates any slack in the printing process.

3.2.3 Printing Files:

Printing files with this method requires the use of the modifications on the printer to be mounted, gel and bath materials to be created, and lastly an offset calibration for the length of the needle used (**fig 13**).

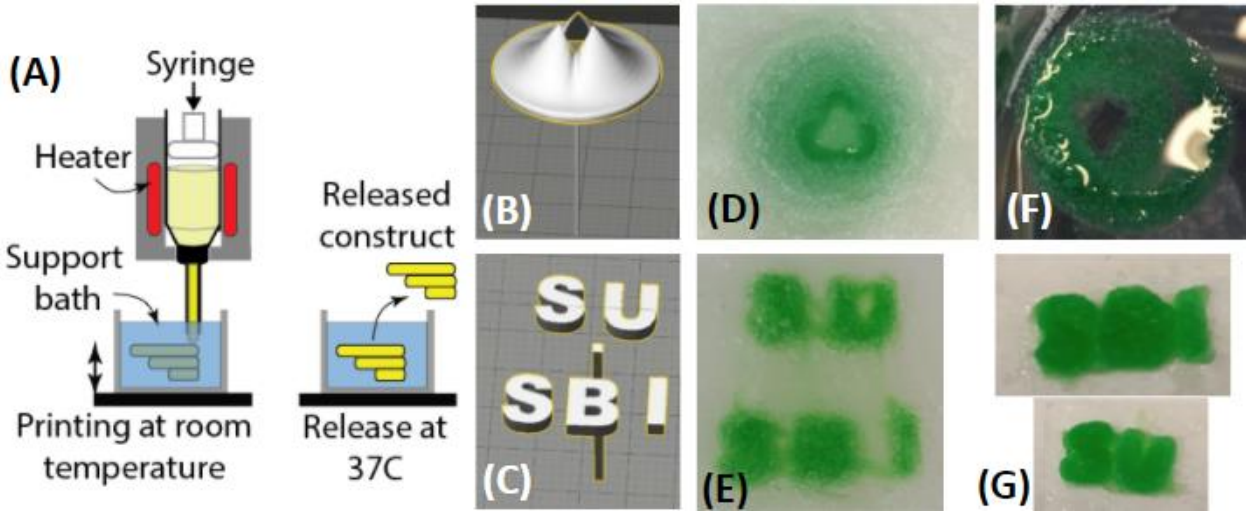

Figure 13: *(A) An overall schematic of the bath based method of injecting the liquid alginate ink into the semisolid bath material to make models. (B) A rendering of a tricuspid valve with an offset underneath. (C) A 3D rendering of SU SBI (Syracuse University, Syracuse Biomaterials Institute). (D) The printed heart valve encased in solid bath material. (E) The SU SBI letters encased in the solid bath material. (F)Once the bath was warmed to 37C the bath gel turns to a liquid releasing the construct. (G) The SU SBI letters were released and then fully separated from the gel material.*

The bath based printing method can be executed by using the following steps: the motor must be plugged in, and the syringe needs to be purged by pressing the Load Filament button on the printer until the screw begins to push material out of the needle. The needle should be mounted on the syringe and used to measure the length it extends to get the exact offset. Offsets have been accounted for a 1” needle, the measurement that is needed is the length the needle extends below the original Z depth of the extruder head.

To account for the offset, add a line to the bottom of the file (in the z-axis) that is just greater than the offset so that the object appears to be floating in the air. The line must extend

less than 200 microns in both the X and Y direction, so that the slicer program does not render G-code with an e (extrusion) value for those locations, causing the file to automatically move to the correct height (Z). The needle should then be removed immediately before the print file can be executed. This must be performed by the user; after the platform goes through the offset, they should pause the program and mount the needle into the gel bath. Afterwards, the user need not interfere with the system. Once everything is loaded and the needle is in the bath the file should print exactly as it is shown on the MakerBot Desktop application.

Note: These are the operations of the post-modified version of the replistruder, the pre-modified version requires modification of the slicer program so that the machine extrudes at a much higher rate than normal, and requires modifications in the X and Y coordinates because the original mount has X, Y offsets as well as a Z offset.

3.3 Difficulties, Optimizations, & Alterations

The main difficulties were twofold; first the device was not very user friendly; it required a lot of customization for every cad file used. Second the device was not very consistent (jamming failing etc.). Occasionally the machine would stop printing either because the gear mechanism was caught or because the alginate solution crosslinked inside the syringe needle causing a jam. Furthermore, during normal operations there were imperfections in the printed replistruder files that caused the rod to oscillate while running and not run concentric. The plastic parts that the rod sits in also had problems with repeated use as they eventually wore out and either stuck to the rod or lost threading altogether and required replacements.

The goal in addressing each of these concerns was to fix them in a mechanically sound way that was also simple to execute and follow so that alterations could be easily replicated. The first problem addressed was the ease of use. To use the original replistruder, various slicer

programs were needed to set the feed rates very high. To simplify this problem, we calculated the proper gear ratio that was needed to extrude the amount of alginate solution desired without manipulating the software. This meant that with the parts printed as is and the slicer that came with *MakerBot* printers, the device was fully functional. By foregoing the software manipulation in lieu of design modifications our goal was to mitigate complexity of operation.

The next hurdle was the friction between the gears and the body, this was fixed by using PTFE (Teflon). A Teflon washer was cut and placed between the moving gears and the body, this eliminated much of the friction and reduced jamming in the gears. Next a delrin spacer was cut on a lathe that could fit the inner diameter of the body. This would make the rotation smoother and more concentric, eliminating wobble in the screw. In addition, since the gear ratios were inverted the small gear was now the main driving gear that pushed the screw. The delrin spacer was placed under the small central gear to align it with the large gear and reduce friction.

A major change was in the way the device was mounted to the machine. The mount we designed, did not require the use of the collar on the end of the device, and more importantly maintained X, Y displacement with the old extruder nozzle position with the only discrepancy being in the Z direction. This was accomplished by creating a mount that not only held the motor, but the entire model in line with the old extruder set up. Ensuring that the syringe was not cantilevered in space and making the prints have a higher fidelity. This is significant because it means that no additional calibrations are needed post installation except for setting the Z offset.

The last modification made was changing the rod to an acme screw and placing a nut on the main drive gear so the plastic wouldn't contact the moving parts, eliminating the need to replace parts when they wore out. A major difference here is that an acme screw will also not

wear on the screw itself, because the shape of the threads is not wedged, and therefore holds up much better under repeated use and cyclic loading.

3.3.1 Gelma Hybrid Ink

After validating that the alginate ink worked and could print complex structures, the next step was to create an ink that was 50% the original alginate mixture (8% NaAlg and 2% collagen) and 50% a gelma mixture (10% GelMa and .25% LAP). The goal here was to use the physical crosslinking of the NaAlg and the calcium ions to physically hold the mixture in a solid state, until specimens could be exposed to UV light and then be held together via chemical crosslinking, giving the structures greater rigidity and altering their physical properties. This ability to alter physical properties becomes important in the simulation of the extracellular matrix (ECM) of different tissues to aid in cellular differentiation.

3.4 Results & Discussion

The alterations that were made to the device improved operation and made use much easier. The process was simplified to only needing to export the file to an SD card, load the syringe with the material to extrude, mount the modified head, and execute the print once the bath was in place. This cut down a lot of software manipulation that was needed beforehand, while the mechanical upgrades greatly reduced the tendency for the machine to jam.

Calibration cubes and other basic shapes were used to gauge reliability and resolution at first, then increased in complexity to biological structures. Custom drawings and scaling were used to make sure that user defined structures were easy to make. Following that, Saos-2 cells were put in the alginate solution to test if the combination of mechanical stresses and chemical concentrations stressed cells enough to cause a cytotoxic reaction. Lastly, the same process was

repeated with a heart valve as the file to make sure that things with curvature and biological application could be created.

To gauge cellular viability a one day live dead test was conducted. Cells were left to sit for a day, after which time they were examined to determine how many were alive and how many were dead via GFP and N3 staining (**fig 14**).

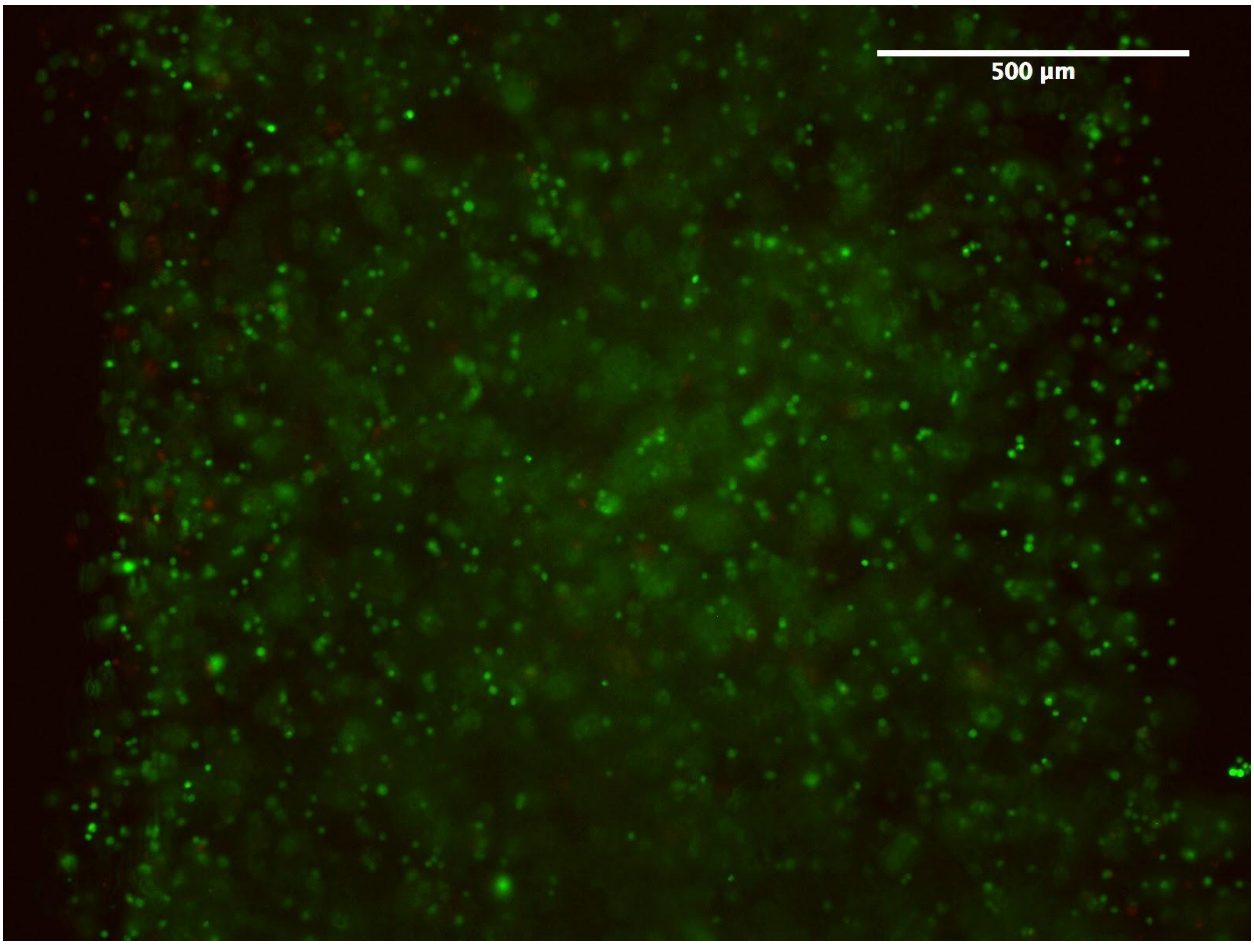

Figure 14: *One day live dead test after printing using the bath method. Living cells fluoresce a green color while dead cells fluoresce red.*

The experiment showed that cell death was incredibly minimal if at all present in any of the trials, meaning that this method may be appropriate for extrusion based biomanufacturing procedures. However, it is important to note that the results may at least partially be from cell type, therefore these results cannot be extended to all cases for all cell types.

The sacrificial bath material worked because it had unique rheological properties that defined it as a Bingham plastic. This means that at low flow regimes it acts like a solid holding the alginate in place, but when the needle pushes through the emulsion it flows around it like a liquid. Without this special property, this printing method would not work.

Another metric by which the success of the printer modifications could be measured was in repeatability. Once the above procedure was set and the parts were modified, prints were successful eight out of an attempted 10 prints with the two exceptions being from a needle clog and a slipped gear. Before the modifications, the print success-failure rate was 30% (3/10), due to problems with tuning the feed rates, and crosslinking in the needle resulting in clogs.

The third parameter that we used to measure the success or failure of our modifications to the replistruder was in terms of how accurate it performed in each configuration. The replistruder was mounted in its usual configuration with the parts provided using the procedures outlined by CMU, and a calibration file was printed in the bath material. This process was repeated after the modifications were made as well to compare any overall differences. The file was a 20mm x 20mm calibration cube (with a 5mm thickness). The original configuration made a cube that was 19mm x 19mm, and after modifications it printed a 19.65mm x 19.65mm. This shows an overall improvement of 3.2% in terms of precision.

The Hybridized ink was tested and analyzed qualitatively but no quantitative testing could be done to measure changes in elasticity, therefore the only result is that it was printed, and could be crosslinked after printing as hypothesized.

This is one in a series of projects to bring 3D bioprinting to the Syracuse Biomaterials institute. A project that was done in conjunction with this one was the use of 3 precision linear actuators and a precision syringe pump to create a printer from scratch with greater accuracy and

precision. A future project involves finding a way to print without the use of sacrificial bath material or in the air. An improvement to the latter would be to use a different crosslinking process as alginate physical crosslinking can be somewhat constraining in terms of the allotment of different materials that can be used.

This project was the first step to making in lab bioprinters by allowing us to 3D print cell encased scaffolds to study how they behave in a 3D environment, and it did just that. My hope is that this work helps future bioprinting attempts in the Syracuse Biomaterial Institute.

3.5 Conclusions

This chapter in the paper centers on the modification and improvement of a technique that was developed at another university. As a result, much of the work that was done was to reduce failure rates, and enhance utility. This was achieved by the addition of machined parts, and embedded acme nuts that eliminated part jamming and wearing on plastic parts respectively. Inversion of the drive gear and driven gear eliminated a significant number of processing requirements for printing. While the use of a custom mount aided in constant offsets for each print. Utility was increased using a ultraviolet dopant that could change the chemical and physical properties of the alginate based ink. This method overall was effective in creating biological designs, however, it required the use of a large amount of sacrificial material. In future endeavors, we seek to remove this nee

Chapter 4: Dual Extrusion Air-based (3D) Printing (DEAP) and Single Extrusion Air-based (3D) Printing (SEAP)

4.1 Introduction

The ability to print soft hydrogels with commercial 3D printers is a huge step with or without the addition of human cells, and something that we have shown to be doable with the use of bath based printing methods. However, in the field of tissue engineering there remains a couple of difficult hurdles to overcome. One being that to create a tissue scaffold two or more different cell types need to be printed in the same construct, and any bulk tissue will require vasculature to prevent necrotic cores from forming. Bath based printing can create very accurate tissue engineering scaffolds out of hydrogels and cells, however, struggles remain to create fine vasculature, and to print two cell types concurrently in the same structure. The SEAP and DEAP methods of 3D printing aim to change that by examining previous adaptations that have been made, finding the factors that hold them back, and eliminating those limitations to allow 3D printers to handle multiple materials at the same time with vasculature (**fig 15**).

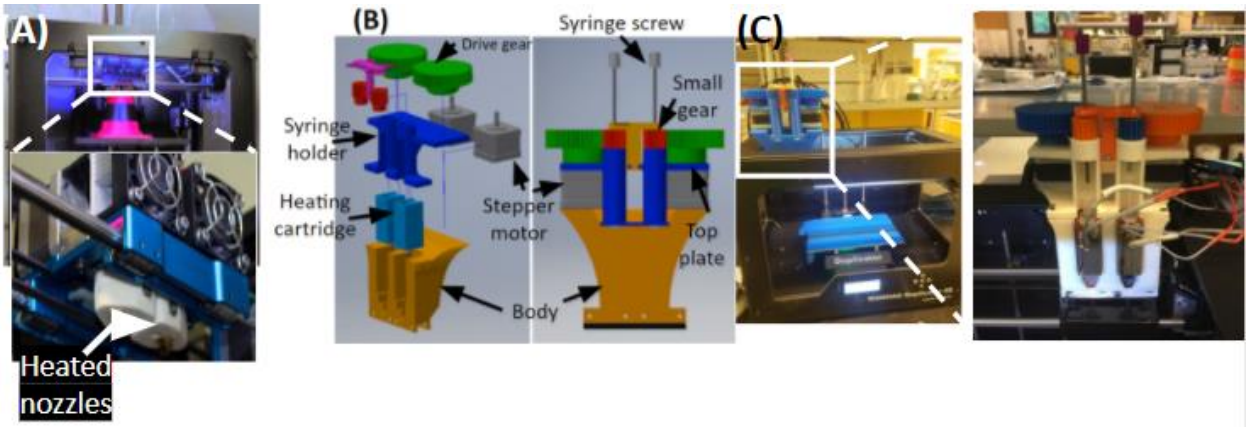

Figure 15:*(A) Unmodified two headed printer setups with two motors and print heads mounted next to one another. (B) Exploded view of cad models for the DEAP models and assembled view. (C) The printed and assembled modification mounted to the same printer as in Figure12A as a drop-in replacement for the regular head.*

Thus far the modifications made to ordinary FDM 3D printers have allowed for the added utility of printing biocompatible polymers, doped polymers, and alginate based inks (with and without human cells). These modifications fall short in that they cannot be executed concurrently, and the soft hydrogels cannot be printed inside of a prepared volume (bath). These limitations needed to be addressed by creating a new process that could be done without the use of a bath, thereby eliminating size limitations, as well as relying on a different phase change mechanism that would happen without the presence of ions. Due to these pre-requisites, this new method could share a common mechanical deposition method (syringe based), however, it would require a completely different phase change method for the soft gel extrusion, meaning a new chemistry with new inks, as well as a two-headed printing method that would allow for concurrent extrusion of dissimilar materials.

This new modality for the 3D printer would require a complete redesign of the mechanical extrusion system. Instead of starting with open source files and modifying them to work more efficiently, we took the lessons from the bath based extrusion portion (gear ratios, nut insets, etc.) and created an entirely new design that had these factors in mind, and was more modular for even easier use and setup. The modular design was key in order to use multiple kinds of inks, reduce load times, and print dissimilar materials (thermoplastics and hydrogels).

4.2 Design & Fabrication

Dual Extrusion Air-based Printing (DEAP) and Single Extrusion Air-based Printing (SEAP) are techniques we developed to 3D print multiple types of cells without the use of a sacrificial bath materials. A vast majority of the design work done between these two methods is the same, as both use the same parts. A major hurdle to overcome was to find a way to print hydrogel material without the use of a bath. The reason not to use a bath stems from the

restrictions that the bath places on the process. These restrictions include chemical; as inks must be alginate based. Volumetric, as whatever was to be printed needed to fit inside the volume of the bath, and lastly, material based restrictions as only one material could be printed at a time. As the name implies the technique involves a modification of a two-headed printer that allows both heads to be turned into independent syringe based extruders. The design used allowed for both heads to be replaced and used independently, however they would have an exact offset from one another since they were part of one solid piece (**fig 16**).

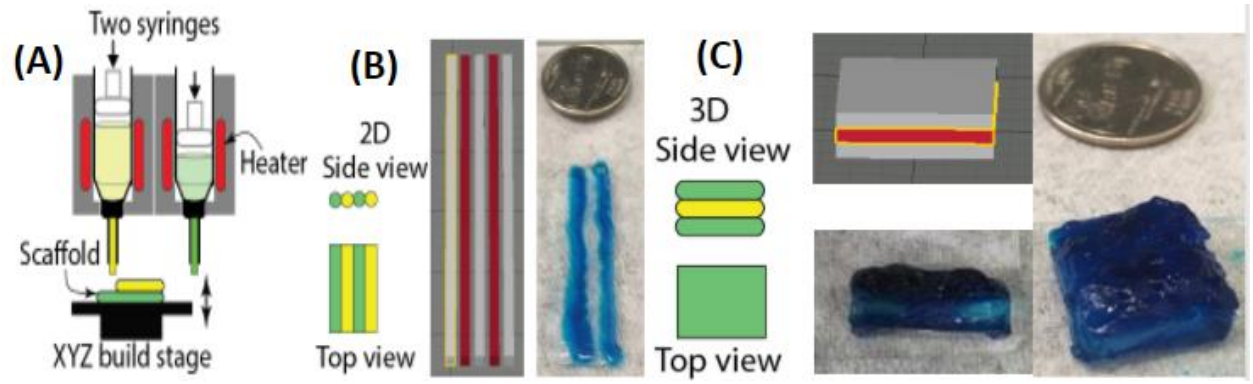

Figure 16: *(A) Diagram showing how the DEAP process works and is capable of printing two materials at the same time. (B) Here you can see the cad file and the output print from the same cad file. The lines are 30mm in length. (C) Here the same cad file to physical object picture is present, except the focus here was to print different materials in Z height layers to create objects.*

The design encompassed a body that serves as both a holder for the syringes, as well as a preset mount so that 1.5" syringe needles would sit flush with the X-Y plane, and the initial head of the printer making calibration the same as for normal printing operations. The next piece that was designed was a top plate that would hold the two stepper motors in place as well as provide placements for the four main gears, and stabilize shafts for the syringe plungers. One of the major lessons learned from modifying the bath based printer was the gears. They were designed such that the turning rates used for 1.75mm filament would work to deposit a volumetric rate of bio-ink comparable to the volume of molten filament that would be left behind normally. This

gear ratio had to originally be calculated during the bath printing modification and was based on the radius of the motor drive shaft, and the number of steps per revolution (212). Since a 6-32 acme screw was used in both machines, the same gear ratio could be used. Where the second machine differs is that the gears themselves could be made larger to make mounting acme nuts much easier. The designed gear ratio, combined with the design of the body enables both the Z axis calibration and feed rates to remain completely unchanged. This process is expanded on in the following diagram (**fig 17**).

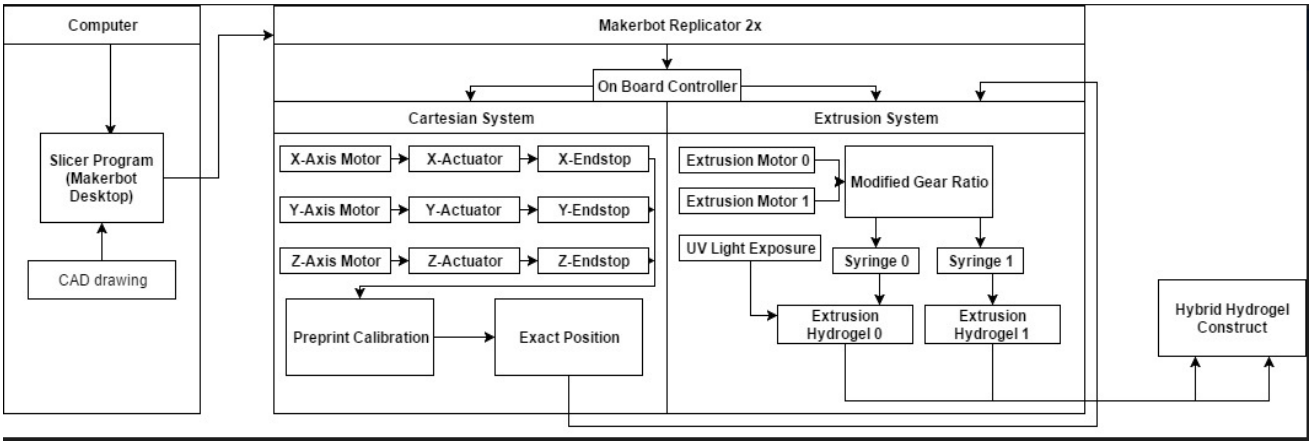

Figure 17: *Process flow diagram showing the flow of data from a central computer into the printer.*

The last parts designed are the gear stay, and the inserts. The gear stay was relatively simple as its only purpose is to mount to the top plate and hold the driven gears in place. The inserts on the other hand were a greater challenge to design and build as they are the only parts that had to be made of metal. It was a point of this project that every part be easy to fabricate, and thus easier to access. With that goal in mind, every other part could be 3D printed from the machine, and then mounted on the machine. This would not work for the inserts because they were required to conduct heat to keep the GelMa ink in a liquid state, while inside the syringe. For this reason, they were made from machinable brass, a material with good conductivity and heat capacitance. They were made by cutting a billet of brass into a 1.00”x0.75”x0.60” cuboid

then boring a major diameter of 0.520.” This would be wide enough to slip the syringe body in, while holding it in place (roughly 0.009” clearance), after that a separate hole was drilled toward the inward corner of the block. The minor hole was 0.250” to fit the heating cartridge of the printer. Lastly, a threaded hole was drilled into the front face of the block to mount the thermocouple that is already equipped to the printer (3m screw thread). The purpose for machining the insert was to be able to use the heating system already built into the printer and use the high thermal conductivity of the brass to accurately control the heat of the ink we were using at all times. Controlling the heat allows us to maintain an environment that cells can thrive in, as well as making the ink less viscous and the printing process easier.

4.3 Advantages & Disadvantages

The advantages to this technique are; it allows for a wider variety of materials to be used so long as they can change phase based on temperature, it forgoes the bath method and therefore has no volumetric limitations, and lastly it can print two cell types at the same time with 200 micron precision directly next to one another. The drawbacks to this technique are that many of the inks being printed require ultraviolet cross-linking to fully set, and are temperature dependent initially to solidify the inks when printed in this method; which somewhat hurts the resolution and clarity of the prints. Inks printed this way rely on temperature to change phase (from 37c to 23c), and this change takes time allowing surface interactions between the glass substrate that the ink is printed on and the ink itself. These interactions cause the surface angle between the gel and the glass to approach zero while the gel is still a liquid, thus causing the fluid to run before it fully solidifies. This “running” of the fluid causes rounded edges and decreased precision. This is the greatest drawback to air based printing methods.

4.4 Process

Printing with this method is very simple as much of the design was based around needing as few changes as possible. The head is already calibrated; gear ratios are already preset to use the original flow rates of the thermoplastic, and the inserts act as cartridges making loading easy. To print with the DEAP method, the insert cartridges need to be loaded with syringes containing the inks to be printed, then slotted into the front of the body. Lastly, the 18g blunt end needles can be loaded from the bottom with a twist, after which the entire printing procedure is the same as dual extrusion printing normally is. There is no need for Z offset calibration or slicer manipulation other than specifying which areas are to be made of what type of ink.

4.5 Single (Bio-) Extrusion Air-based (3D) Printing (SEAP) Differences

Single bio-extrusion 3D printing may seem to be a step backward from the dual model; however, this was a technique that allowed us to print thermoplastics and bio-inks at the same time (**fig18**).

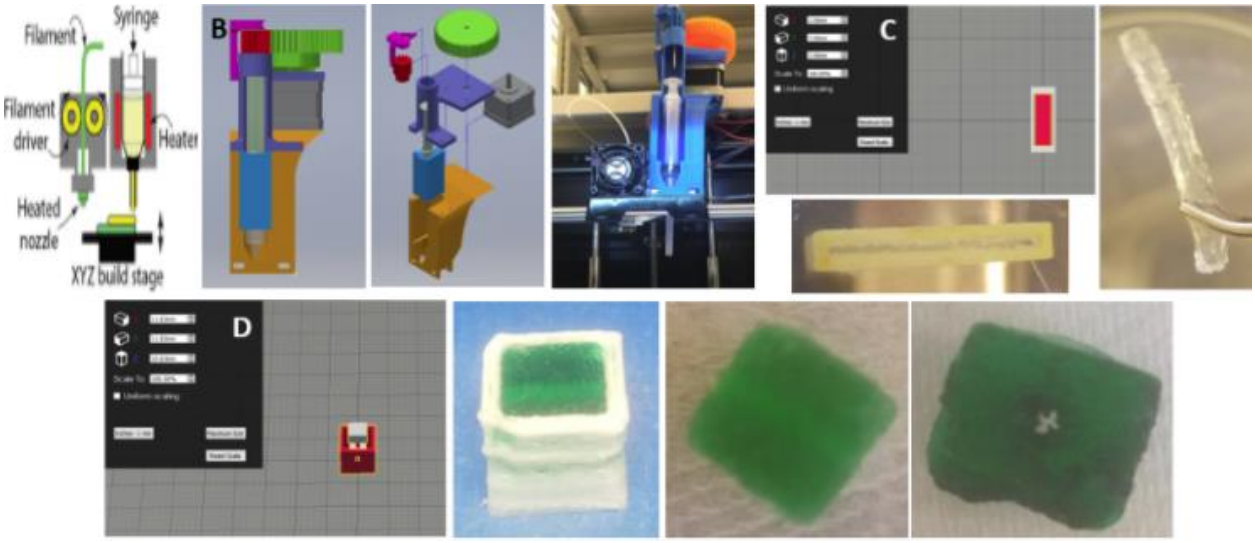

Figure 18: *(A) Diagram of how the SEAP method prints two dissimilar materials at the same time. (B) exploded and assembled view of the SEAP design model as well as the mounted model on a printer. (C) In this print, we needed to create rectangular lines with good precision so this method was chosen to increase precision. (D) The cad file and printing of a cube with a vessel inside it. This vessel is created by printing a sacrificial material inside the GelMa (PVA).*

The single refers to the number of inks that can be used at a given time in the process; however, the modification itself is done to a *MakerBot Replicator 2X*. This gives us the utility of a second head that is unmodified to print a variety of thermoplastics both biodegradable and sacrificial. This is the third and final modification that we designed and the novelty is that we can

print materials with such dissimilar properties at the same time right alongside one another. In our initial test print we used polyvinyl acid (PVA) as a sacrificial shell in which we printed one of our inks, a mixture of GelMa and gelatin, in the middle of which we could print the inner lumen of a vessel through the gel. This technique allows us a great deal of variability with what we can print. You could print one layer of a sacrificial thermoplastic, and the next a cell laden bioink, and after the printing process the sample can be crosslinked with ultraviolet light, and then submerged in warm water to dissolve away the sacrificial material (**fig 19**).

Figure 19: A cartoon representation of SEAP with the PVA represented in yellow and gelma in the green. As you can see this method can be used to create luminal vasculature.

The strengths to this process are that it gives us the greatest versatility in printing, i.e. we can use any material on this set up; thermoplastic or bioink, and any dopant we would like. Printing PVA alongside hydrogels also gives the benefit of creating an outer shell that helps prevent the bleeding effect that the gel has as it cools by providing a solid boundary. Another benefit is the ability to print biodegradable polymers alongside, and within our hydrogel constructs that can provide cells a surface to adhere to as well as other chemical dopants. Another strength to this modification is that it did not require making an entire mechanical design from scratch. All the parts used for this process were the original DEAP parts partitioned in the middle with only two exceptions. The gear stay and top plate had to be slightly modified to counteract a moment force placed on the gear stay by only having force applied on one side, therefore another bolt hole was added and a ridge to stabilize the gear stay and the acme screw.

The downsides to this process are minimal; however there have been some issues that require the machine to print the thermoplastic layer just above the hydrogel layer. This must be done to prevent clogging in the thermoplastic nozzle as contact with the hydrogel was found to drastically reduce the temperature at the print head and cause clogging. The fix for this was simply to elevate the hydrogel portion 200 microns from the build plate, then increase the perceived diameter of the filament that is being printed on the *MakerBot* Desktop application. By doing this the machine will automatically print the thermoplastic first (as it is touching the platform), then it will print the hydrogel section just above that layer. Then by increasing the perceived filament diameter and going into the head of the machine that we modified; the printer will extrude slightly less, thereby reducing the bleeding effect of the cooling bioink. This trick works because the 3D printers have an internal program to let them know how much filament to extrude at any given time. The basics of this program are that the machine always thinks that the filament being fed into it is 1.75mm. From there it takes the steps per revolution of the Nema 17 stepper motor, 212, and the diameter of the main drive gear in the primary configuration. From here based on the radius of the drive gear the machine knows that each step of the motor corresponds to an amount of rotation at the end of the drive gear, and assuming no slipping, it then knows the linear feed rate of the filament with a 1.75mm cross sectional diameter. By squaring the radius of the cross section of the filament and multiplying by pi we get the volumetric flowrate that the machine bases its accuracy and precision. Therefore, by making the machine think that a larger piece of filament is being fed into the head it will reduce the rate that it feeds that filament in order to maintain the same volumetric flow rate, however we're not actually feeding that volume, therefore we will get a more anemic flow rate. This was the same analysis that had to be done to calculate the gear ratios for all the other modifications. The end

nozzle of the head is 400 microns, however, there are other controls to elongate the filament as it's being printed that the machine will automatically implement as it moves in a given XY plane (i.e. when it tries to make rounded edges, it has to slow down and avoid drastic accelerations). These are all automatically done by the *MakerBot* Desktop software and help in printing of any material including our bioinks. The following diagram illustrates the process a bit more clearly (**fig 20**).

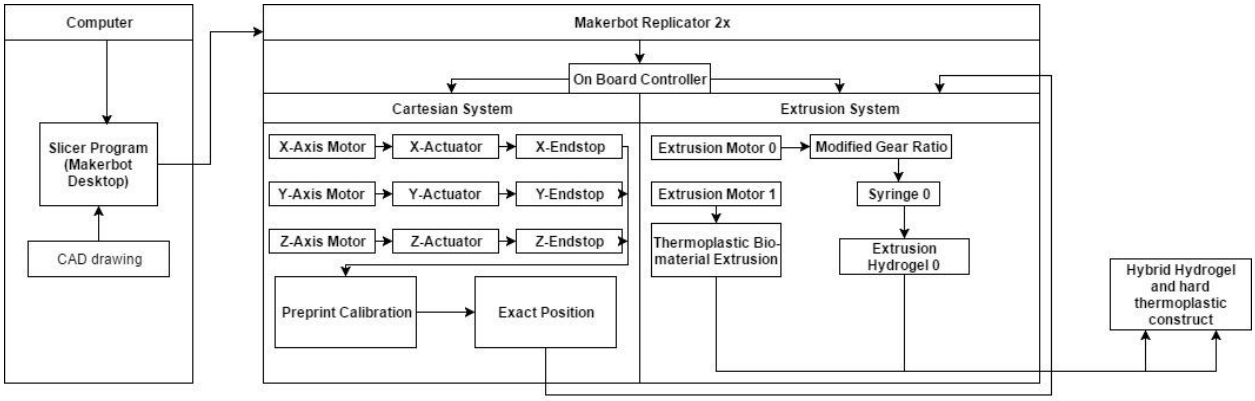

Figure 20: *The process flow diagram of the SEAP process, the only difference between the SEAP and DEAP methods come in the extrusion system.*

4.6 Results

As a result of finding a method that could print soft hydrogels and biocompatible polymers the DEAP and SEAP designs were created, and fabricated. Both methods succeeded in overcoming the obstacles that were presented. The DEAP model could print without the use of a bath and multiple hydrogel materials concurrently; a modality that was previously absent from the bath based method. The SEAP method loses the ability to print two soft materials concurrently but adds the ability to print two dissimilar materials, including sacrificial thermoplastics thus increasing the fidelity of prints and gaining access to the ability to print vasculature within bulk constructs. These added modalities are both novel and address two of the main problems associated with creating tissue engineering scaffolds.

References

[1] Liu Y, Lim J, Teoh S-H. Review: development of clinically relevant scaffolds for vascularised bone tissue engineering. Biotechnology advances 2013;31:688-705.

[2] Domb AJ, Kost J, Wiseman D. Handbook of biodegradable polymers: CRC Press; 1998.

[3] Hutmacher DW. Scaffolds in tissue engineering bone and cartilage. Biomaterials 2000;21:2529-43.

[4] Atala A. Engineering tissues, organs and cells. Journal of tissue engineering and regenerative medicine 2007;1:83-96.

[5] Tarik Arafat M, Gibson I, Li X. State of the art and future direction of additive manufactured scaffolds-based bone tissue engineering. Rapid Prototyping Journal 2014;20:13-26.

[6] Trachtenberg JE, Mountziaris PM, Miller JS, Wettergreen M, Kasper FK, Mikos AG. Open-source three-dimensional printing of biodegradable polymer scaffolds for tissue engineering. Journal of Biomedical Materials Research Part A 2014;102:4326-35.

[7] Chevalier E, Chulia D, Pouget C, Viana M. Fabrication of porous substrates: A review of processes using pore forming agents in the biomaterial field. Journal of Pharmaceutical Sciences 2008;97:1135-54.

[8] Peltola SM, Melchels FP, Grijpma DW, Kellomäki M. A review of rapid prototyping techniques for tissue engineering purposes. Annals of medicine 2008;40:268-80.

[9] Billiet T, Vandenhaute M, Schelfhout J, Van Vlierberghe S, Dubruel P. A review of trends and limitations in hydrogel-rapid prototyping for tissue engineering. Biomaterials 2012;33:6020-41.

[10] Williams JM, Adewunmi A, Schek RM, Flanagan CL, Krebsbach PH, Feinberg SE, et al. Bone tissue engineering using polycaprolactone scaffolds fabricated via selective laser sintering. Biomaterials 2005;26:4817-27.

[11] Cooke MN, Fisher JP, Dean D, Rimnac C, Mikos AG. Use of stereolithography to manufacture critical-sized 3D biodegradable scaffolds for bone ingrowth. Journal of Biomedical Materials Research Part B: Applied Biomaterials 2003;64:65-9.

[12] Patrício T, Domingos M, Gloria A, D'Amora U, Coelho J, Bártolo P. Fabrication and characterisation of PCL and PCL/PLA scaffolds for tissue engineering. Rapid Prototyping Journal 2014;20:145-56.

[13] Tuan HS, Hutmacher DW. Application of micro CT and computation modeling in bone tissue engineering. Computer-Aided Design 2005;37:1151-61.

[14] Wei C, Cai L, Sonawane B, Wang S, Dong J. High-precision flexible fabrication of tissue engineering scaffolds using distinct polymers. Biofabrication 2012;4:025009.

[15] Hutmacher DW, Sittinger M, Risbud MV. Scaffold-based tissue engineering: rationale for computer-aided design and solid free-form fabrication systems. Trends in biotechnology 2004;22:354-62.

[16] Gratson GM, García-Santamaría F, Lousse V, Xu M, Fan S, Lewis JA, et al. Direct-write assembly of three-dimensional photonic crystals: conversion of polymer scaffolds to silicon hollow-woodpile structures. DTIC Document; 2005.

[17] Wang F, Shor L, Darling A, Khalil S, Sun W, Güçeri S, et al. Precision extruding deposition and characterization of cellular poly-ϵ-caprolactone tissue scaffolds. Rapid Prototyping Journal 2004;10:42-9.

[18] Park SH, Park DS, Shin JW, Kang YG, Kim HK, Yoon TR, et al. Scaffolds for bone tissue engineering fabricated from two different materials by the rapid prototyping technique: PCL versus PLGA. Journal of Materials Science: Materials in Medicine 2012;23:2671-8.

[19] Bose S, Vahabzadeh S, Bandyopadhyay A. Bone tissue engineering using 3D printing. Materials Today 2013;16:496-504.

[20] Nichol JW, Koshy ST, Bae H, Hwang CM, Yamanlar S, Khademhosseini A. Cell-laden microengineered gelatin methacrylate hydrogels. Biomaterials 2010;31:5536-44.

[21] Soman P, Chung PH, Zhang AP, Chen S. Digital microfabrication of user-defined 3D microstructures in cell-laden hydrogels. Biotechnology and bioengineering 2013;110:3038-47.

[22] Sun M, Downes S. Physicochemical characterisation of novel ultra-thin biodegradable scaffolds for peripheral nerve repair. Journal of Materials Science: Materials in Medicine 2009;20:1181-92.

[23] Shor L, Güçeri S, Wen X, Gandhi M, Sun W. Fabrication of three-dimensional polycaprolactone/hydroxyapatite tissue scaffolds and osteoblast-scaffold interactions in vitro. Biomaterials 2007;28:5291-7.

[24] Swetha M, Sahithi K, Moorthi A, Srinivasan N, Ramasamy K, Selvamurugan N. Biocomposites containing natural polymers and hydroxyapatite for bone tissue engineering. International journal of biological macromolecules 2010;47:1-4.

[25] Rho J-Y, Kuhn-Spearing L, Zioupos P. Mechanical properties and the hierarchical structure of bone. Medical engineering & physics 1998;20:92-102.

[26] Bakhshinejad, Ali, and Roshan M. D'Souza. "A Brief Comparison between Available Bio-printing Methods." *2015 IEEE Great Lakes Biomedical Conference (GLBC)* (2015): n. pag. Web.

[27] Chisti, Yusuf. "Hydrodynamic Damage to Animal Cells." Critical Reviews in Biotechnology 21.2 (2001): 67-110. Web.

[28] Cive, and Fluid Mechanics and Properties of Fluids. 1. Fluids Mechanics and Fluid Properties (n.d.): n. pag. Web.

[29] E., and Rev. Roum. Chim. Http://web.icf.ro/rrch/ RHEOLOGICAL PROPERTIES OF SODIUM ALGINATE SOLUTIONS (n.d.): n. pag. Web.

[30] "Extruder." Encyclopedia Britannica Online. Encyclopedia Britannica, n.d. Web. 18 May 2016. Website

[31] Funami, Takahiro. "Rheological Properties of Sodium Alginate in an Aqueous System during Gelation in Relation to Supermolecular Structures and Ca2+ Binding." Rheological Properties of Sodium Alginate in an Aqueous System during Gelation in Relation to Supermolecular Structures and Ca2+ Binding. Food Hydrocolloids, Oct. 2009. Web. 19 May 2016.

[32] "Synthesis and Degradation Rheology and Extrusion." Advances in Polymer Science (1982): n. pag. Web.

[33] Lien, Sheng-Chien. "Mechanical Regulation of Cancer Cell Apoptosis and Autophagy: Roles of Bone Morphogenetic Protein Receptor, Smad1/5, and P38 MAPK." *Mechanical Regulation of Cancer Cell Apoptosis and Autophagy: Roles of Bone Morphogenetic Protein Receptor, Smad1/5, and P38 MAPK*. N.p., n.d. Web. 26 May 2016.

[34] Joshi, Sunil C., Y.c Lam, F.y.c Boey, and A.i.y Tok. "Power Law Fluids and Bingham Plastics Flow Models for Ceramic Tape Casting." *Journal of Materials Processing Technology* 120.1-3 (2002): 215-25. Web.

[35] "Bilby3D : Tech Support." *BilbyCNC Tech Support Article- How to Clean the Drive Gear :*. N.p., n.d. Web. 26 May 2016.

[36] "How A Ball Screw Works." *How a Ball Screw Works*. N.p., n.d. Web. 26 May 2016.

[37] "Replistruder Syringe-Based Extruder." *NIH 3D Print Exchange*. N.p., n.d. Web. 31 May 2016.

[38] "Dennis J. McHugh, CHAPTER 2 - PRODUCTION, PROPERTIES AND USES OF ALGINATES."*CHAPTER 2 - PRODUCTION, PROPERTIES AND USES OF ALGINATES*. N.p., n.d. Web. 31 May 2016.

[39] "Evaluation of the Nitroaldol Reaction in the Presence of Metal Ion-crosslinked Alginates†." N.p., n.d. Web.

[40] Park, Jennifer S., Julia S. Chu, Anchi D. Tsou, Rokhaya Diop, Zhenyu Tang, Aijun Wang, and Song Li. "The Effect of Matrix Stiffness on the Differentiation of Mesenchymal Stem Cells in Response to TGF-β."*Biomaterials*. U.S. National Library of Medicine, 01 June 2011. Web. 01 June 2016.

[41] Heino, J. "Result Filters." *National Center for Biotechnology Information*. U.S. National Library of Medicine, n.d. Web. 01 June 2016.

[42] Kleinman, H. K. "Role of Collagenous Matrices in the Adhesion and Growth of Cells." *The Journal of Cell Biology* 88.3 (1981): 473-85. Web.

[43] "0x7D.com." *0x7Dcom*. N.p., n.d. Web. 01 June 2016.

[44] Kim, Nayoun, and Seok-Goo1 Cho. "Clinical Applications of Mesenchymal Stem Cells." *The Korean Journal of Internal Medicine*. The Korean Association of Internal Medicine, 1 July 2013. Web. 01 July 2016.

[45] Lee, Kangwon, Eduardo A. Silva, and David J. Mooney. "Growth Factor Delivery-based Tissue Engineering: General Approaches and a Review of Recent Developments." *Journal of the Royal Society Interface*. The Royal Society, 06 Feb. 2011. Web. 05 July 2016.

[46] Thomson JA, Itskovitz-Eldor J, Shapiro SS, Waknitz MA, Swiergiel JJ, Marshall VS, Jones JM (1998). "Blastocysts Embryonic Stem Cell Lines Derived from Human". *Science* **282**(5391): 1145–1147. Bibcode:1998Sci… 282.1145T.doi: 10.1126/science.282.5391. 1145. PMID 9804556.

[47] Schöler, Hans R. (2007). "The Potential of Stem Cells: An Inventory". In Nikolaus Knoepffler; Dagmar Schipanski; Stefan Lorenz Sorgner. *Humanbiotechnology as Social Challenge*. Ashgate Publishing. p. 28. ISBN 978-0-7546-5755-2.

[48] Guan K; Nayernia K; Maier LS; Dressel, Ralf; Lee, Jae Ho; Nolte, Jessica; Wolf, Frieder; Li, Manyu; Engel, Wolfgang; Hasenfuss, Gerd; et al. (April 2006). "Pluripotency of spermatogonial stem cells from adult mouse testis". *Nature* **440** (7088): 1199–203.Bibcode:2006Natur.440.1199G. doi:10.1038/nature04697. PMID 16565704.

[49] Ibelgaufts, Horst. "Cytokines & Cells Online Pathfinder Encyclopedia accessed 7/7/16

[50] Reilly, G. C., and A. J. Engler. "Result Filters." *National Center for Biotechnology Information*. U.S. National Library of Medicine, n.d. Web. 07 July 2016.

[51] Trappmann, B. "Result Filters." *National Center for Biotechnology Information*. U.S. National Library of Medicine, n.d. Web. 07 July 2016.

[52] Mironov, V. "Organ Printing: Tissue Spheroids as Building Blocks." *National Center for Biotechnology Information*. U.S. National Library of Medicine, n.d. Web. 08 July 2016.

[53] Hegen, Anja, Anna Blois, Crina E. Tiron, Monica Hellesøy, David R. Micklem, Jacques E. Nör, Lars A. Akslen, and James B. Lorens. "Efficient *in Vivo*Vascularization of Tissue Engineering Scaffolds." *Journal of Tissue Engineering and Regenerative Medicine*. U.S. National Library of Medicine, Apr. 2011. Web. 09 July 2016.

[54] DesRochers, Teresa M., Laura Suter, Adrian Roth, and David L. Kaplan. "Bioengineered 3D Human Kidney Tissue, a Platform for the Determination of Nephrotoxicity." *PLoS ONE*. Public Library of Science, 2013. Web. 09 July 2016.

[55] Sanyal, Ph.d. Suparna. "Culture and Assay Systems Used for 3D Cell Culture." *Culture and Assay Systems Used for 3D Cell Culture* (n.d.): n. pag. Web.

[56] Yarmush, M. L. "Hepatic Tissue Engineering: Development of Critical Technologies." - *YARMUSH*. N.p., n.d. Web. 11 July 2016.

[57] "Swiss Alp Health - SCIENCE." *Swiss Alp Health - SCIENCE*. N.p., n.d. Web. 14 July 2016.

Vita

Lucas Albrecht was an undergraduate student at Syracuse University from the year of 2011 graduating with a bachelors in bioengineering in 2014. He then began his Master's studies with supervisor Pranav Soman. This paper is the culmination of the research conducted during his graduate studies in tissue engineering and 3D printing. The author also worked on many other projects while in the laboratory including shape memory auxetic 3D printing, microvasculature in hydrogels and biologically inspired mechanical scaffolding for mechanical engineering applications.